Zoological Journal of the Linnean Society, 2023, **XX**, 1–22
https://doi.org/10.1093/zoolinnean/zlad168
Advance access publication 8 December 2023
Original Article

Original Article

Species delimitation and phylogenetic analyses of a New Guinean frog genus (Microhylidae: *Hylophorbus*) reveal many undescribed species and a complex diversification history driven by late Miocene events

Flavien Ferreira[1,*], Fred Kraus[2], Stephen Richards[3], Paul Oliver[4], Rainer Günther[5], Wahyu Trilaksono[6], Evy Ayu Arida[7], Amir Hamidy[6], Awal Riyanto[6], Burhan Tjaturadi[8], Christophe Thébaud[1], Philippe Gaucher[9] and Antoine Fouquet[1]

[1]Laboratoire Evolution et Diversité Biologique, UMR 5174, CNRS, IRD, Université Paul Sabatier, Bâtiment 4R1, 118 Route de Narbonne, 31062 cedex 9 Toulouse, France
[2]Department of Ecology and Evolutionary Biology, University of Michigan, Ann Arbor, MI 48109, USA
[3]Herpetology Department, South Australian Museum, North Terrace, Adelaide, Sout Australia 5000, Australia
[4]Centre for Planetary Health and Food Security, Griffith University, 170 Kessels Road, Brisbane, Queensland, 4111, Australia
[5]Museum für Naturkunde, Leibniz-Institut für Evolutions- und Biodiversitätsforschung, Invalidenstraße 43, 10115 Berlin, Germany
[6]Laboratory of Herpetology, Museum Zoologicum Bogoriense, Research Center for Biosystematics and Evolution, National Research and Innovation Agency (BRIN), Gd. Widyasatwaloka, Jl. Raya Jakarta Bogor km 46, Cibinong, West Java, Indonesia
[7]Research Center for Applied Zoology, National Research and Innovation Agency (BRIN), Gd. Widyasatwaloka, Jl. Raya Jakarta Bogor km 46, Cibinong, West Java, Indonesia
[8]Center of Environment Studies, Sanata Dharma University, Yogyakarta, Indonesia
[9]Laboratoire Ecologie, Evolution, Interactions des Systèmes Amazoniens (LEEISA), USR3456, Cayenne, French Guiana

[Version of Record, published on: http://zoobank.org/urn:lsid:zoobank.org:pub:C205A49A-A66E-466E-8D6D-CBA702798B0A]

[*]Corresponding author. Laboratoire Evolution et Diversité Biologique, UMR 5174, CNRS, IRD, Université Paul Sabatier, Bâtiment 4R1, 118 Route de Narbonne, 31062 cedex 9 Toulouse, France. E-mail: flavienferreira1@gmail.com

ABSTRACT

New Guinea is the largest tropical island in the world and hosts immense endemic biodiversity. However, our understanding of how the gradual emergence of the terrestrial ecosystems of the island over the last 40 Myr has generated this biological richness is hampered by poorly documented species diversity and distributions. Here, we address both these issues through an integrative taxonomy and biogeographical approach using *Hylophorbus*, a New Guinea-endemic genus of frogs with 12 recognized species. We delimited candidate species by integrating mitochondrial DNA, nuclear DNA, and bioacoustics, then investigated their evolutionary history. Our results suggest that the current taxonomy of the genus misses true species diversity by ≥3.5-fold. Nevertheless, most candidate species (27) remain unconfirmed because of missing data, whereas five were identified unambiguously as undescribed (we describe three of these formally). Time-calibrated phylogenetic analyses suggest that *Hylophorbus* diversification began ~9 Mya in the northern or eastern portion of New Guinea. It would appear that lineages dispersed to new terrestrial habitats in the west, notably uplifted by the central range orogeny, until eventually reaching the Bird's Head during the Mio-Pliocene (7–5 Mya). Conversely, a past barrier appears to have prevented north–south dispersal. These data suggest that new habitat availability has primarily driven the diversification of *Hylophorbus*.

Keywords: amphibian; biogeography; cryptic species; Indo-Pacific; 16S ribosomal RNA; island fauna; phylogeography; alpha taxonomy

INTRODUCTION

Although biodiversity is declining worldwide at a fast pace (Ceballos *et al.* 2017, 2020), our understanding of basic metrics, such as the number and distribution of species, remains vastly incomplete for many groups, particularly in the tropics (Giam *et al.* 2012). This knowledge shortfall implies that an unknown proportion of biodiversity might vanish before being documented (McDonald *et al.* 2022). Moreover, the dearth of knowledge is

Received 12 January 2023; revised 3 October 2023; accepted 17 October 2023

such that it jeopardizes macroevolutionary inferences in many groups (Utami *et al.* 2022). This applies especially to large tropical forested regions, such as Amazonia (Vacher *et al.* 2020), the Congo Basin (van Ginneken *et al.* 2017, Jongsma *et al.* 2018), and New Guinea (NG) (di Marco *et al.* 2017), the latter being the largest tropical island on Earth (786 000 km^2) and one of the least-studied regions in the world (Beehler and Laman 2020). Although species richness and endemism are known to be spectacularly high in NG (Dinerstein and Wikramanayake 1993, Myers *et al.* 2000, Cámara-Leret *et al.* 2020), comprehensive diversity estimates are currently lacking owing to a lack of island-wide data in all taxonomic groups except birds (Brito 2010, Kennedy *et al.* 2022). This is largely attributable to the rugged topography (e.g. central range mountain chain extending 1300 km longitudinally and peaking at ≤4800 m) but also to the sparse infrastructure and logistical issues that render biological surveys challenging and irregular.

The geographical structure of NG biodiversity is insufficiently documented to understand fully the relationship between the geodynamic evolution of the region and the diversification processes that took place within the island. Nevertheless, available data suggest that biotic diversification in NG is relatively recent in comparison to other species-rich tropical regions. The first terrestrial ecosystems may date back to the late Palaeogene (~40–25 Mya) with the emergence of a proto-Papuan archipelago (Hall 1998, 2009, Davies 2012), the remnants of which now form most of the Papuan Peninsula (easternmost part of NG; Fig. 1). Most *in situ* diversification events seem to have taken place during even more recent periods (last 15 Myr) in a vast array of taxonomic groups, including flowering plants (*Schefflera* Forst JR and Forst G 1775; Shee *et al.* 2020), tree-kangaroos (*Dendrolagus* Müller 1840; Eldridge *et al.* 2018), rodents (Hydromyini Gray 1825; Roycroft *et al.* 2022), birds (Meliphagidae Vigors 1825, *Goura* pigeons Stephens 1819, Melanocharitidae Sibley and Ahlquist 1985; Marki *et al.* 2017, Bruxaux *et al.* 2018, Milá *et al.* 2021), lizards (*Papuascincus* Allison and Greer 1986, *Cyrtodactylus* Gray 1827, and *Hypsilurus* Peters 1867; Tallowin *et al.* 2018, 2020, Slavenko *et al.* 2020), diving beetles (*Exocelina* Balke 1998; Toussaint *et al.* 2014, 2021), and frogs (Asterophryinae Günther 1858; Oliver *et al.* 2013, 2017, Rivera *et al.* 2017, Hill *et al.* 2022). This tempo of diversification is consistent with current orogenic models, according to which NG acquired its modern configuration during the Mio-Pliocene (7–5 Mya), notably with the uplift of the central range (from ~5.5 Mya according to Hill and Hall 2003; vs. 15–5 Mya according to Quarles van Ufford and Cloos 2005). Therefore, despite differences in their ecology and variation in the estimated times of NG colonization, it seems that the diversification of most of these lineages was facilitated by progressively emerging landmasses.

Many questions remain about the spatial and temporal aspects of the emergence of NG, in particular those involving the westernmost part of the island, known as the 'Bird's Head' (BH) or 'Vogelkop peninsula'. This geologically composite region results mostly from an east–west collision between a drifting sliver that detached from the Australian craton (Supporting Information, Fig. S1) and the proto-Papuan archipelago (Bailly *et al.* 2009, Baldwin *et al.* 2012, Davies 2012). This part of the island clearly hosts a wide range of endemic taxa (Marshall and Beehler 2007), but its terrestrial biota is currently less documented than the rest of NG. Therefore, it remains unclear how this region has contributed to the evolutionary and biogeographical history of NG, with some studies portraying the BH as a source of diversity (e.g. Unmack *et al.* 2013, Georges *et al.* 2013) and others as a sink (e.g. Toussaint *et al.* 2021).

Figure 1. Topographic map of New Guinea displaying the sampling localities (red dots). Names of mountain ranges are in italic.

Amongst vertebrates, amphibians stand out as having generally restricted spatial distributions and particularly low dispersal abilities (Duellman *et al.* 1999). As a corollary, their diversification is tightly linked to major palaeogeographical and climatic events (Zeisset and Beebee 2008, Smith *et al.* 2017, Ortiz *et al.* 2023). As a consequence, they represent a useful model group to test hypotheses regarding spatiotemporal diversification underlying present-day terrestrial diversity patterns across NG. Asterophryinae is the main amphibian lineage in NG and its satellite islands (≥14 genera and 323 recognized species; Frost 2023), and the species diversity could be conjectured to be at least three times larger than what is depicted by current taxonomy (Köhler and Günther 2008, Arida *et al.* 2021).

Within Asterophryinae, *Hylophorbus* Macleay 1878, is a dazzling example of the taxonomic knowledge gap affecting NG. The genus was believed to be monotypic until the turn of the 21st century (Günther 2001) but currently includes 12 recognized species (Frost 2023), each characterized by a narrow distribution range. The overall narrow range of each species, the island-wide distribution of the genus from sea level to 2000 m a.s.l. (Zweifel 1972, Günther 2001), and the existence of many populations with highly divergent mitochondrial DNA (mtDNA) lineages that cannot be assigned to any taxa (e.g. Arida *et al.* 2021) suggest that many *Hylophorbus* spp. remain to be discovered, described, and named. Recent phylogenomic studies have recovered a *Mantophryne* Boulenger 1897 + *Hylophorbus* clade and estimated that the diversification of *Hylophorbus* occurred within the last 10 Myr (Feng *et al.* 2017, Hime *et al.* 2021, Portik *et al.* 2023). Given the phylogenetic relationships recovered in previous papers (Rivera *et al.* 2017, Tu *et al.* 2018, Hill *et al.* 2023, Portik *et al.* 2023), the genus might have started to diversify within the northern terranes, which include the northern mountain ranges of NG (Fig. 1; Supporting Information, Fig. S1), and dispersed from there to the BH region at least twice (Tu *et al.* 2018, Portik *et al.* 2023). The timing of these events seems to coincide with the expansion of terrestrial habitat in NG (see above). However, these inferences are based on limited sampling, with only a few *Hylophorbus* representatives, and might therefore be based upon a low portion of the species diversity of this genus.

Here, we investigate the temporal and spatial aspects of the diversification of *Hylophorbus* after re-evaluating the diversity within the genus, a prerequisite to drawing meaningful biogeographical inferences in such a poorly known region and animal group. We acquired biological material and molecular data throughout the range of the genus and tested the congruence between mtDNA, nuclear DNA (nuDNA), and bioacoustic analyses to delimitate lineages that could correspond to putative species (i.e. an integrative taxonomy approach; Dayrat 2005, Padial *et al.* 2010). We then obtained a time-calibrated phylogeny based on multiple loci to test whether: (i) *Hylophorbus* started to diversify in the northern terranes, followed by dispersal events occurring westwards to the BH; (ii) the BH has been colonized at least twice; and (iii) the central range acted as a barrier during *Hylophorbus* diversification.

MATERIALS AND METHODS

Taxon and genetic sampling

This study includes 109 samples of *Hylophorbus* for molecular data, of which 63 are newly analysed and 46 are represented by GenBank sequences only (Supporting Information, Table S1). Note that four *Hylophorbus* specimens identified as *Cophixalus* sp. in GenBank (TNHC54754, TNHC-GDC31221, TNHC51333, and CCA) were re-identified as *Hylophorbus* sp. based on previous phylogenomic work (Feng *et al.* 2017, Tu *et al.* 2018). Our sampling comprises all the recognized species of *Hylophorbus*, with the exception of *Hylophorbus sigridae* Günther *et al.* 2014, and includes samples distributed throughout the range of the genus (44 localities; Fig. 1). Genomic DNA was extracted from muscle or liver tissues using the Wizard® Genomic DNA Purification kit (Promega Corporation, Madison, WI, USA), following the manufacturer's instructions.

The DNA dataset (~3500 bp) contains three mitochondrial (*12S* ribosomal DNA and two disjunct *16S* ribosomal DNA loci referred to as *16S* 'a' and 'b') and three nuclear (*Tyr*, *BDNF*, and *C-Myc*) loci (Supporting Information, Table S2). All *Hylophorbus* sequences available on GenBank for these loci (131) were retrieved, and the rest were obtained by PCR (for protocol, see Supporting Information, Appendix S1; for details of loci and primers, see Supporting Information, Table S2) and Sanger sequencing (Eurofins Genomics, EU). Consensus sequences were generated after chromatogram checks in Geneious R9.1.7. Finally, 31 *12S*, 30 *16S*a, 62 *16S*b, 33 *Tyr*, 28 *BDNF*, and 30 *C-Myc* newly generated sequences were obtained (Supporting Information, Table S1). GenBank and new sequences were aligned using MAFFT v.7 (Katoh *et al.* 2019), following the E-INS-i method for mitochondrial loci and default parameters for nuclear loci. Each alignment was verified, notably the coding loci reading frames, in Geneious R9.1.7, and 100% identical flanking regions were eliminated while conserving a region represented by ≥50% of all terminals (Supporting Information, Table S2). Finally, we built a mtDNA-only dataset using all available terminals (109) to delimit molecular operational taxonomic units (MOTUs), in addition to a mt + nuDNA loci dataset formed by a single terminal for each MOTU (44) to analyse their phylogenetic relationships. All the new sequences are available in GenBank (Supporting Information, Table S1), and the mtDNA-only and mt + nuDNA datasets are available on OSF (https://doi.org/10.17605/OSF.IO/XVJQU).

Species delimitation

Mitochondrial DNA-based species delimitation

We first delimited MOTUs based on mtDNA data, using three complementary single-locus delimitation methods: (i) the automatic barcode gap discovery (ABGD; Puillandre *et al.* 2012) based on *16S*a and *16S*b; (ii) the single-rate Poisson tree processes (PTP; Zhang *et al.* 2013) using the concatenated mtDNA matrix (1862 bp); and (iii) the generalized mixed Yule coalescent approach (GMYC; Pons *et al.* 2006, Monaghan *et al.* 2009), also using the concatenated mtDNA matrix. The sister genus *Mantophryne* was chosen as an outgroup for all delimitations (Oliver *et al.* 2013, Feng *et al.* 2017, Hime *et al.* 2021); the methods are detailed in the Supporting Information (Appendix S2). The final MOTUs were defined according to a consensus established by the majority rule, i.e. defined as any lineage supported by at least two of the three methods. In cases of two different ABGD delimitations, the most conservative one in terms of the number of species was adopted.

Nuclear DNA differentiation

To assess the congruence of differentiation between the mtDNA-based MOTUs and nuclear data, we produced median-joining networks of each nuDNA locus (Bandelt and *et al.* 1999) using POPART v.1.7 software (Leigh and Bryant 2015). Allele networks are often used in species delimitation to test allele sharing among mtDNA-based groups (e.g. Leaché *et al.* 2009, Fouquet *et al.* 2022), when using only a few loci is not informative enough to test boundaries among candidate species through tree-based methods (cf. maximum likelihood trees of the nuDNA loci in Supporting Information, Fig. S2).

Sixteen MOTUs of the 44 delimited (see the Results section) were represented by all three nuclear loci, 14 by two, five by one, and nine by none (Supporting Information, Table S1). MOTUs sharing alleles on two or more loci were considered in the same nuDNA partition because allele sharing among closely related MOTUs is indicative of current or recent interbreeding or of shared ancestral polymorphism. Conversely, in the case of MOTUs not sharing alleles on at least two loci, we considered the mtDNA and nuDNA differentiation as congruent.

Bioacoustics

Bioacoustic variation and its congruence with the DNA-based delimitation was investigated using 21 recordings of *Hylophorbus*, representing six recognized species (11 recordings), and four MOTUs from individuals not yet assigned to any taxon (10 recordings). In addition, data provided in the original descriptions of eight species (Günther 2001, Richards and Oliver 2007, Kraus and Allison 2009, Günther *et al.* 2014) were also included in the acoustic analyses, leading to a total of 31 call recordings involving 10 recognized species (21 recordings).

Five variables were measured using means based on all notes and calls of each recording, following the note-centred approach of J. Köhler *et al.* (2017): dominant frequency, note duration, inter-note interval, number of notes per call, and number of pulses per note, defined as the number of energy bursts of ~100% per note. Frequency modulation within notes was coded as '1' and absence as '0' in the dataset (Supporting Information, Table S3). The variables were measured manually in AUDACITY v.3.1.3 (Audacity Team 2022), and sonograms were generated using the R package 'Seewave' (Sueur *et al.* 2008). Variation was examined through a principal component analysis in R using the 'factoextra' package (Kassambara and Mundt 2020). We considered an absence of overlap among multidimensional space representing MOTUs as confirming the candidate species genetic delimitation (note that, in cases of singletons that were not outliers in the principal component analysis, the different call characteristics were examined individually to assess the distinctiveness of MOTUs).

Integrative taxonomy

Following the candidate-species approach of Vieites *et al.* (2009) and Padial *et al.* (2010), we tested the congruence between mtDNA-based MOTUs, nuDNA, and bioacoustic data, in order to reach an integrative diagnosis of the delimited MOTUs. First, in cases of genetic differentiation and bioacoustic differentiation, MOTUs were considered confirmed candidate species (CCS). Second, in cases of no genetic differentiation but distinctiveness on bioacoustics, MOTUs were considered false negatives and CCS. Third, in cases of genetic differentiation but absence of clear differences on bioacoustics, MOTUs were defined as deep conspecific lineages (DCL), i.e. false positives. Fourth, in cases of missing data preventing us from reaching any integrative diagnosis, MOTUs were considered as unconfirmed candidate species (UCS).

Linking *Hylophorbus rufescens* Macleay 1878 with our delimited MOTUs remained ambiguous. Therefore, we defined *Hylophorbus* cf. *rufescens* as represented by the specimens ABTC42916, LSUMZ94942, and LSUMZ94943 (for justification, see Supporting Information, Appendix S3). We treat *Hylophorbus rufescens myopicus* Zweifel 1972 and *Hylophorbus rufescens extimus* Zweifel 1972 as valid species, following Kraus (2021), because their morphological diagnosability (Zweifel 1972), insularity, and distance from the type localities of all the other *Hylophorbus* species make it clear that they are independently evolving lineages that meet the unified species concept (de Queiroz 2007). *Hylophorbus sigridae* is possibly the only species out of all recognized *Hylophorbus* taxa missing in our molecular sampling. We are confident that no MOTU could correspond to this taxon because its call is distinctive from the calls of the MOTUs for which acoustic data are available, and because its type locality (Muller Range; −5.7291, 142.2632) is distant (257 km minimum) from the closest occurrence of unassigned MOTUs. Finally, at least one type of data is available for all *Hylophorbus* taxa, whether it is DNA or bioacoustics.

Time-calibrated phylogeny

To infer phylogenetic relationships and divergence times among *Hylophorbus* lineages, we selected one individual of each of the 44 delimited MOTUs (see the Results section) and four outgroup species (*Choerophryne proboscidea* van Kampen 1914, *Sphenophryne cornuta* Peters and Doria 1878, *Callulops robustus* Boulenger 1898, and *Mantophryne lateralis* Boulenger 1897) based on the phylogeny of Tu *et al.* (2018) and the availability of sequences in GenBank. We used the six loci previously described (*12S*, *16S*a, *16S*b, *Tyr*, *BDNF*, and *C-Myc*) to generate four partitions (one for the concatenation of mtDNA and one for each nuDNA locus). The best-fitting evolutionary models for each partition (Supporting Information, Table S4) were selected using IQTREE MODELFINDER (Chernomor *et al.* 2016, Kalyaanamoorthy *et al.* 2017), according to the Bayesian information criterion (BIC).

We reconstructed a time-calibrated tree in BEAST v.2.5 using a birth–death tree prior. Divergence time estimation was implemented using an uncorrelated relaxed lognormal clock model for each partition (Drummond and Rambaut 2007). Two time calibration priors were set with uniform distributions (Schenk 2016): (i) the most recent common ancestor (MRCA) of *Choerophryne* van Kampen 1914 and *Hylophorbus*, bounded between 17.4 and 12.8 Mya (Hime *et al.* 2021) and (ii) the MRCA of *Mantophryne* and *Hylophorbus*, bounded between 15.2 and 10.1 Mya (Feng *et al.* 2017). We did not use monophyly constraints, considering previous uncertainties regarding the monophyly of some Asterophryinae genera (Rivera *et al.* 2017). Two MCMC chains of 50 million iterations were generated, with a pre-burn-in of 10% (a posteriori burn-in of 10%) and subsequently combined with LOGCOMBINER v.2.5 (Bouckaert *et al.* 2014). The convergence was evaluated according to the effective

sample size (ESS), all of which were > 200. Finally, the maximum clade credibility tree was obtained using TreeAnnotator v.2.5 after analysing 9000 trees (Drummond and Rambaut 2007).

Biogeographical analyses

The ultrametric subtree obtained from the multilocus analysis including *Hylophorbus* + *Mantophryne* was analysed with the R package BioGeoBEARS (Matzke 2018). This allowed us to infer ancestral distribution areas using maximum likelihood. Three different models, and their variants with the jumping dispersal parameter (J), were tested: dispersal–vicariance (DIVA; Ronquist 1997); dispersal–extinction–cladogenesis (DEC; Ree and Smith 2008); and BayAREA (BAYES; Landis *et al.* 2013). As implemented by Matzke (2018), these models similarly allow processes such as dispersal–vicariance, extinctions, or within-area speciation (DEC and BAYES only). Although some biases concerning the J parameter have been debated [notably, its tendency to underestimate the contribution of anagenetic dispersal events (Ree and Sanmartín 2018)], its utility is still asserted (Matzke 2021). Therefore, we have considered the models with and without 'J', with the best scores [based on the Akaike information criterion (AIC); Supporting Information, Table S5], and results from both were compared. Finally, non-adjacent ranges were disallowed for the analyses. Five biogeographical zones were defined based on the geological history of NG and its palaeogeography (for details about each region, see Supporting Information, Appendix S3): (i) the northern terranes; (ii) the Australian craton; (iii) the BH; (iv) the Papuan Peninsula; and (v) The 'Woodlark' (Woodlark island + D'Entrecasteaux islands) and Louisiade Archipelagos.

RESULTS

Species delimitation

Mitochondrial DNA

Of the three species-delimitation methods, ABGD was the most conservative, recovering a total of 38 MOTUs based on the consensus between the *16S*a and *16S*b delimitation of 35 and 32 MOTUs, respectively (Supporting Information, Fig. S3). We selected partitions forming plateaus in the number of delimited MOTUs (P = .0092–.0239 for *16S*a and .0025–.0148 for *16S*b). These values are close to thresholds found in other vertebrates (Puillandre *et al.* 2012). The GMYC delimitation led to the largest number of MOTUs (48) and the PTP to an intermediate number (44 MOTUs). The different partitionings are highly congruent overall, with the majority consensus recognizing 44 MOTUs (Fig. 2A; Supporting Information, Fig. S3). Four major clades are recovered from the mtDNA tree (Fig. 2A; Supporting Information, Fig. S3). Interestingly, their distribution overlaps only in the BH (clades C and D) and the northern terranes (clades A and C), with the exception of *Hylophorbus* sp. 'Moroka', which is the only MOTU from the Papuan Peninsula not belonging to clade A (Fig. 2B).

For 69 pairs of MOTUs, the pairwise interspecific genetic distance (p-distance) at the *16S*b locus is <5% (Supporting Information, Table S6); among these, nine pairs have a p-distance of <3%, with a minimum of 1.2%. Pairwise interspecific genetic distance between 3% and 5% for the *16S*b locus are thresholds in amphibians above which distances can indicate interspecific comparisons (Vences *et al.* 2005, Fouquet *et al.* 2007).

Nuclear DNA

The four major clades recovered with mtDNA are also segregated on the *C-Myc* and *Tyr* allele networks (Supporting Information, Fig. S4) and only in part on the *BDNF* network. For all three loci, *Hylophorbus atrifasciatus* Kraus 2013, is unambiguously distinct, as is *Hylophorbus infulatus* Zweifel 1972 on *BDNF*, which mirrors the long branches of these species in the mtDNA tree (Fig. 2A). In contrast, less allelic polymorphism was recovered among closely related MOTUs within clades B, C, and D (Supporting Information, Fig. S4), which mirrors their shorter branches on the mtDNA tree. Notably, the network obtained with *BDNF* harbours several instances of allele sharing among related MOTUs. For all loci, sympatric MOTUs (sharing the same mountain ranges) do not share any allele, which might suggest reproductive isolation. An exception is the range overlap between *Hylophorbus proekes* 'Torricelli' and *Hylophorbus proekes* 'Adelberts', two MOTUs that share an allele on *C-Myc*, which might indicate interbreeding or ancestral polymorphism. Finally, considering the evidence provided by the three nuDNA loci, their consensus is fully congruent with the mtDNA consensus (Fig. 2A; Supporting Information, Fig. S4).

Bioacoustics

The first two axes of the principal component analysis using bioacoustic data account for 61.3% of the variance (Fig. 2C; Supporting Information, Fig. S5). Along these axes, all MOTUs are discriminated, with the exception of *H. proekes* 'Adelberts' and *Hylophorbus picoides* Günther 2001, which overlap along axis 1. However, further analysis focusing on a subset of MOTUs (Fig. 2C) discriminates them all, notably with differences involving note frequency modulation (decreasing for *H. picoides* vs. increasing for *H. proekes* 'Adelberts') and the number of notes per call (one to nine for *H. picoides* and 10–14 for *H. proekes* 'Adelberts') (Table 1; Supporting Information, Fig. S6A, B).

Integrative consensus

The integrative consensus leads us to consider 17 MOTUs as CCS and 27 as unconfirmed (Fig. 2). Five CCS cannot be associated with any existing taxon, which are represented by 12 of the 44 delimited MOTUs, excluding *H.* cf. *rufescens*, which remains a UCS. Three of these five unnamed CCS are named and described in the 'Taxonomic account' section. Interestingly, the new species ***H. lengguru*** and ***H. monophonus***, in addition to *H. proekes* 'Torricelli' and *H. proekes* 'Adelberts', form species pairs based on mtDNA (Fig. 2A) but they display clearly distinct calls (Table 1; Fig. 2C). Furthermore, even in the absence of bioacoustic data for the new species ***Hylophorbus maculatus***, we consider it as a CCS, because: (i) it is genetically distinct from other CCS (Fig. 2; clade C) on both mtDNA and nuDNA (Supporting Information, Figs S3, S4); (ii) it has a distinctively small body size [snout–vent length (SV) = 23.4–24.2 mm; N = 2] that overlaps only with geographically distant species (*H. atrifasciatus*, *Hylophorbus richardsi* Günther 2001, and *H. sigridae*; Supporting Information, Fig. S7A); and (iii) it has a singular spotted pattern on the flanks and venter.

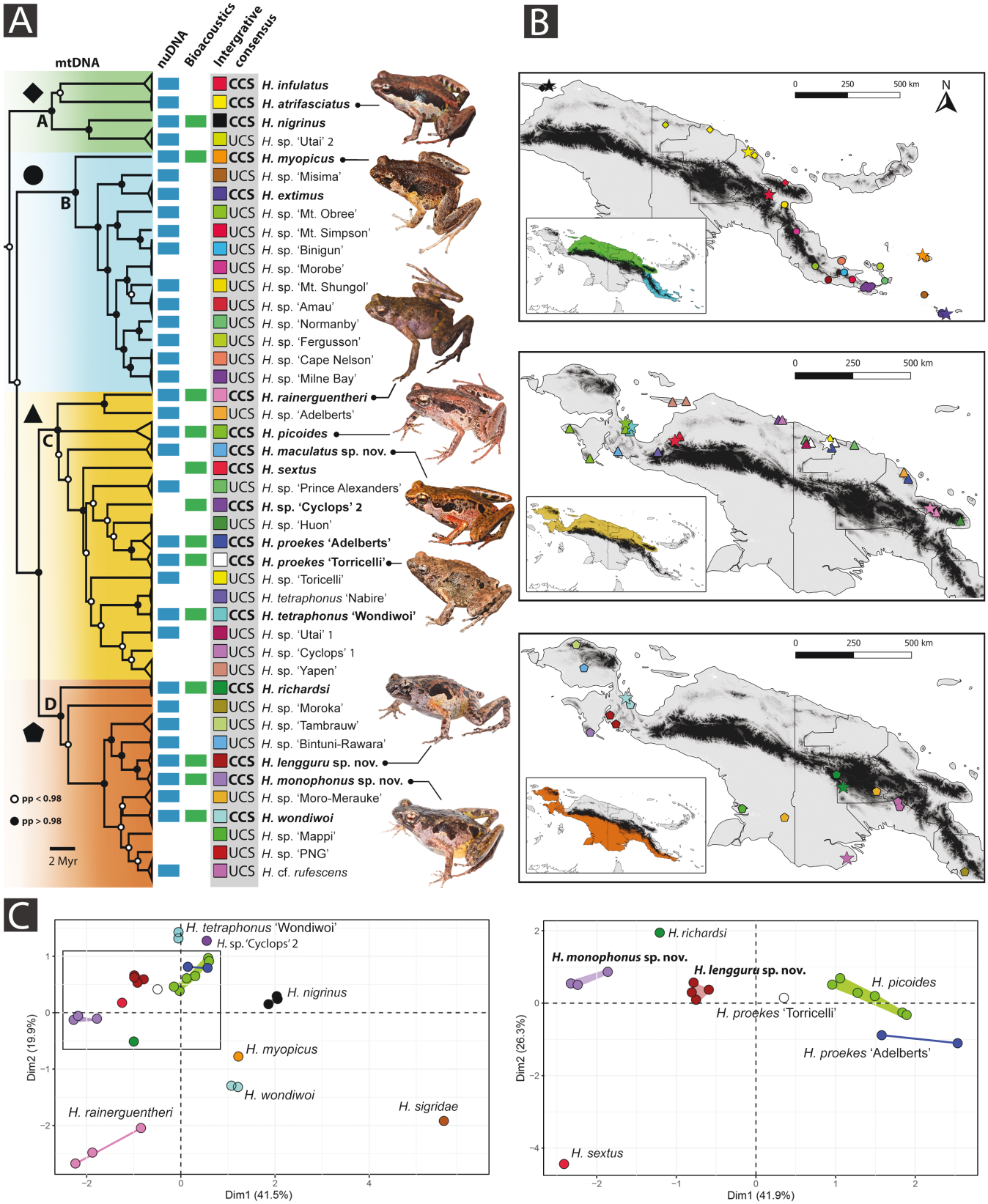

Figure 2. Species delimitation summary figure. A, summary of the integrative species delimitation within *Hylophorbus* comparing mtDNA-based ultrametric tree (BEAST) with collapsed branches for each MOTU (consensus across the three methods used), nuDNA network partitions, and variation in bioacoustics. B, distributions of MOTUs grouped by major clades: clades A, B, C, and D. The maps were generated in QGIS v.2.14; stars correspond to species type localities; coloured areas in the inset maps represent putative distributions of identified clades. C, principal component analyses for *Hylophorbus* bioacoustic variables; left panel, using all call recordings ($N = 31$), and right panel, focused

Table 1. Advertisement call variables across *Hylophorbus* species, presented as ranges and means (in parentheses). The number of calls (*N*) from which the ranges are based is indicated below the species names. Data for each call recording are available in the Supporting Information (Table S3).

Species	Mean dominant frequency (kHz)	Note duration (ms)	Internote duration (ms)	Notes per call	Pulses per note	Mean note repetition rate (s^{-1})
H. lengguru (*N* = 53)	1.13	89–138 (107)	132–208 (163)	2–6 (3.00)	1	4.46
H. monophonus (*N* = 70)	1.27	108–153 (131)	635–2395 (1570)	1	1	.950
H. myopicus (*N* = 3)	1.27	37–111 (81.3)	57–93.0 (69.3)	9–10 (9.75)	2–4 (2.80)	7.36
H. nigrinus[a] (*N* = 14)	1.96	62–101 (86.5)	44–51.0 (48.3)	9–13 (12.0)	1	7.71
H. picoides[a] (*N* = 72)	1.48	72–91 (80.7)	146–163 (153)	1–9 (5.00)	2	5.14
H. proekes 'Torricelli'[a] (*N* = 9)	1.02	98–137 (104.4)	123–141 (135)	5–7 (6.00)	1–4 (2.20)	4.20
H. proekes 'Adelberts' (*N* = 8)	1.22	104–196 (122)	103–158 (131)	10–14 (11.7)	2–6 (2.20)	3.10
H. rainerguentheri[a] (*N* = 45)	1.10	69–120 (297)	1310–2800 (2170)	1	1	.510
H. richardsi (*N* = 2)	1.40	60–61 (60.5)	1600	1	1	1.14
H. sextus[a] (*N* = 8)	1.40	143–211 (185)	101–220 (167)	2–3 (2.50)	1	3.38
H. sigridae[a] (*N* = 5)	1.60	22–42 (37.2)	51–99 (64.3)	18–20 (19.0)	1	10.2
H. sp. 'Cyclops' 2 (*N* = 1)	1.79	74–82 (81.8)	87–143 (125)	6	1	5.58
H. tetraphonus 'Wondiwoi'[a] (*N* = 61)	1.75	81–132 (98.0)	131–238 (160)	1–5 (3.50)	1	4.67
H. wondiwoi[a] (*N* = 44)	1.00	25–61 (49.8)	58.8–71 (63.8)	7–12 (9.30)	1	9.06

[a]Data from original species descriptions were used for data completion.

Phylogenetic analyses and biogeography

The time-calibrated tree based on the mt + nuDNA loci of the 44 selected individuals is presented in Figure 3. *Hylophorbus* forms a strongly supported clade [posterior probability (pp) = 1; Supporting Information, Fig. S8], whose diversification started ~9 Mya (Fig. 3). Four major internal clades are strongly supported (pp = 1). Clade A (node 2: 8.3–5.5 Mya) forms the sister group of the rest of the genus and includes four species from the northern terranes (Fig. 3). Clade B (node 6: 6.1–4.0 Mya) includes species from the Papuan Peninsula and southeastern archipelagos. The clade formed by C + D is strongly supported (pp = 1) and diverged from clade B ~8 Mya. Eight of the 14 nodes with pp < .90 are within clade C, and all these less-supported nodes are estimated to be younger than 5 Myr. Clade C (node 19: 7.2–5.1 Mya) is mostly distributed in the northern terranes but also includes three species from the BH, thus having a distribution overlapping with clades D (node 34: 7.0–4.7 Mya) and A. Clade D includes a single species from

on a subset (*N* = 18) that are clustering together in the complete analysis (black rectangle in the left panel). In A, rectangles in the nuDNA (blue) and bioacoustics (green) column indicate distinctness between MOTUs. The mtDNA-based tree with uncollapsed branches and posterior probabilities (pp) of each node can be seen in the Supporting Information (Fig. S3). In C, note that one specimen of *H. picoides* and one of ***H. lengguru*** are represented by two recordings each (cf. Supporting Information, Table S3); see the Supporting Information (Fig. S4) for correlation circles and loadings of the principal component analyses. Names in bold indicate CCS. The nuDNA partitioning was established according to a majority rule based on the allele networks presented in the Supporting Information (Fig. S4). Consistent colour coding refers to species identity throughout the figure. Abbreviations: CCS, confirmed candidate species; Dim, dimension, i.e. 'Axis'; UCS, unconfirmed candidate species. Photograph credits, from top to bottom: S. Richards (1, 2, 3, 6) and A. Fouquet (4, 5, 7, 8).

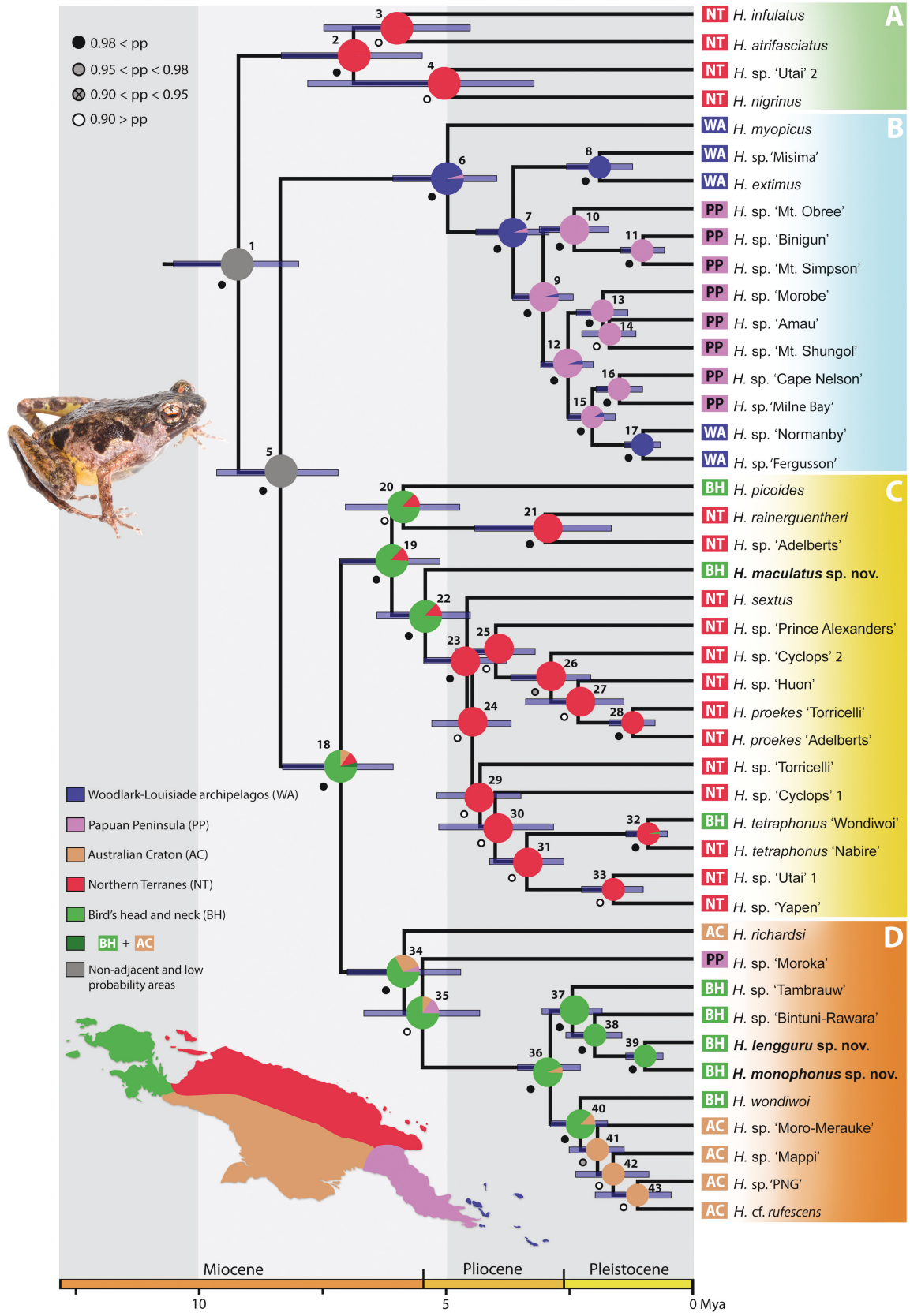

Figure 3. Time-calibrated phylogenetic tree of *Hylophorbus* inferred from the analysis of mitochondrial and nuclear loci (mtDNA: *12S* and *16S*; nuDNA: *Tyr*, *C-Myc*, and *BDNF*), and ancestral areas inferred using BioGeoBEARS under the DIVA+J model (results of the DIVA model are presented in Supporting Information, Fig. S9). Nodal support [posterior probability (pp)] is indicated below the nodes with dots; pp values are presented in the Supporting Information (Fig. S8). Node bars indicate the 95% highest posterior distribution of node dates. Colours in node pie charts refer to geographical area inferences, consistent with the map colours, and grey indicates negligible (<10%) or non-adjacent area inferences. The branch of the outgroup *Mantophryne lateralis* (Papuan Peninsula distribution) has been removed to simplify the figure visually.

the Papuan Peninsula (*H.* sp. 'Moroka'), but all the other species are from the BH and the Australian craton.

The best-fitting biogeographical models according to AIC values are the DIVA and DIVA+J models (Supporting Information, Table S5). There were only minor differences between the inferences of these models (Fig. 3; Supporting Information, Fig. S9). The ancestral range for the MRCA of all *Hylophorbus* remains ambiguous in both models (node 1: 10.5–8.0 Mya; Fig. 3). Diversification within clade A is estimated to have taken place within northern terranes between 8.3 and 3.2 Mya (upper and lower boundary of the highest posterior distribution of node 2 and 4, respectively). Diversification within clade B (node 6) has taken place during the last 6 Myr and implies two dispersal–vicariance events between southeastern archipelagos and the Papuan Peninsula: the first between 6.1 and 4.0 Mya (node 6), which involves the Louisiade islands, then between 1.4 and .70 Mya (node 12), which involves the D'Entrecasteaux islands.

Both the DIVA+J and the DIVA models support the BH as being the ancestral area of clade C + D, thus suggesting an early diversification within western NG, ~7 Mya onwards. The biogeographical origin of both clades C and D is inferred as being in the BH according to the DIVA+J model but remains ambiguous for clade D according to the DIVA model (Supportig Information, Fig. S9). A 3-Myr-old subclade within clade D (node 36) diversified within the BH and dispersed recently towards the Australian craton.

Clade C is the most species rich, and both models suggest a BH origin. However, this result remains ambiguous because of the poorly supported relationships among early branches within the clade (node 20; Fig. 3). However, most of the diversification of this clade unambiguously occurred within the northern terranes during the last 5 Myr and necessarily implies at least one, possibly two, early dispersal events between the northern terranes and the BH (nodes 20 and 22: 8.3–6.1 Mya).

DISCUSSION

Our integrative species delimitation suggests that there could be ≥3.5 times more species of *Hylophorbus* than recognized by current taxonomy, with most species being narrowly distributed. Biogeographical analyses remain ambiguous about the ancestral range of the MRCA of *Hylophorbus*, although they suggest that the genus underwent westward dispersal during the last 7 Myr. We also found support for multiple colonization of the BH, and subsequent *in situ* diversification that led to further dispersal towards the southern part of NG (Australian craton). Finally, we did not recover any dispersal–vicariance event across the central range, advocating for a pre-existing barrier between the northern terranes and the Australian craton.

Integrative taxonomy and species richness

We delimited 44 MOTUs based on mtDNA, including 12 that are already named. Only 5 of the last 32 are confirmed by nuDNA and acoustic data (3 are described in this study), because the remaining 27 lack sufficient data from other lines of evidence to be assessed as other than UCS. This highlights the challenges of achieving comprehensive sampling for anurans in this region, although this is crucial because mtDNA-based species delimitation, when morphological or acoustic data are lacking, is prone to false positives, which can be accentuated by sparse geographical sampling (Sukumaran and Knowles 2017), or false negatives. For example, phenotypically distinct MOTUs can display a degree of genetic differentiation that could be insufficient to delimit two species (e.g. p-distance = 1.2% at the *16S*b locus between ***H. monophonus*** and ***H. lengguru***; Supporting Information, Table S6). However, several UCS were immediately assessed as undescribed species upon capture in the field (F.K., pers. obs.), thus advocating that most of these would be assessed as CCS if calls and morphology were examined.

Despite a lot of missing data in our dataset, our results represent progress in flagging candidate species and identifying missing/available data, such as acoustic and topotypical material, that might foster future taxonomic work. The delimitation of 44 candidate species in this study represents an increase by ~3.5-fold in recognized *Hylophorbus* species diversity. This figure is slightly higher than what could have been expected based on previous works that were based on more limited sampling for the genus (Rivera *et al.* 2017, Arida *et al.* 2021). Moreover, the MOTUs are often limited to single or a handful of spatially circumscribed localities; as a consequence, it is currently difficult to evaluate their distributional range. Nevertheless, our results suggest that most *Hylophorbus* species are narrow-range endemics, as are almost all Asterophyinae species (Oliver *et al.* 2022; Hill *et al.* 2022). Given this pattern of endemism and large sampling gaps (e.g. western portion and northern foothills of the central range, Tamrau Mountains, and Van Rees Mountains), it is probable that many extant species remained unsampled. This degree of knowledge gap in the taxonomy (Linnean shortfall; Hortal *et al.* 2015) is not surprising because most recent integrative studies that have evaluated species diversity of tropical amphibian groups have found a 2- to 6-fold increase in species diversity in comparison to current taxonomy (Fouquet *et al.* 2014, 2021, 2022). Nevertheless, the case of *Hylophorbus* remains particularly striking, with many cryptic species harbouring few diagnostic morphological traits beyond details of colour pattern, but having very distinct calls. These findings highlight the need for integrative taxonomic approaches and improved geographical sampling in poorly studied groups before studying their evolutionary history, and they remind us how partial our current perception of biodiversity is in NG.

Biogeography

Given the potentially large number of species that might be missing in our analyses, possible lineage extinctions, and the moderate support of some of the nodes in our multilocus tree, any inference about the historical biogeography of *Hylophorbus* should be taken with caution. Yet, some unambiguous conclusions can be drawn from our results, in particular those about *in situ* diversification within NG subregions, and sporadic dispersal–vicariance events across regions coinciding with important geological changes of NG.

We initially hypothesized that *Hylophorbus* started to diversify in the northern terranes and found that the diversification of *Hylophorbus* began ~9 Mya, within an ancestral range that remains difficult to characterize. However, we argue that this range was likely to be located in the eastern and/or northern portions of NG for the following reasons: (i) *Mantophryne*, the

sister genus of *Hylophorbus* (crown age ~12.5 Mya) (Hill *et al.* 2022), currently occupies the East Papuan Composite Terrane (i.e. Papuan Peninsula and southeastern archipelagos), from which it is also likely to originate (Oliver *et al.* 2013, Hill *et al.* 2023); (ii) the ancestral range of clade B was inferred as the East Papuan Composite Terrane; (iii) the ancestral range of the early diverging clade A is the northern terranes; and (iv) a BH origin of *Hylophorbus* is incompatible with the nested phylogenetic position of the species occurring in that region. Moreover, this is in line with biostratigraphic data that suggest a connection between the BH landmass and the rest of NG not earlier than 6 Mya (Gold *et al.* 2017). Mid-to-late Miocene origins in the East Papuan Composite Terrane and northern terranes have also been inferred in several other taxonomic groups, such as flowering plants, beetles, skinks, and geckos (Toussaint *et al.* 2014, 2021, Tallowin *et al.* 2018, Shee *et al.* 2020, Slavenko *et al.* 2020). The emergence of new terrestrial habitats in the west, possibly accessible from the accreting northern terranes (Hall 2002, Quarles van Ufford and Cloos 2005), emerging Bird's Neck (Bailly *et al.* 2009, Baldwin *et al.* 2012), and/or west-drifting blocks (Hall 2002, 2012, Hill and Hall 2003, Webb *et al.* 2019), probably enabled multiple dispersal events westwards.

Multiple dispersal–vicariance events between the southeastern archipelagos and the Papuan Peninsula and secondarily back to the southeastern archipelagos are suggested within clade B by our analysis (Fig. 3), a pattern similar to that seen in *Cyrtodactylus* lizards (Tallowin *et al.* 2018). Considering the current bathymetry of this region (seafloor rarely >100 m in depth), and past sea-level fluctuations (Miller *et al.* 2020), land bridges at times of low sea level must have connected some of the islands to one another (Kraus 2015), in addition to some islands to the NG mainland. Overseas dispersal in salt-intolerant organisms, such as anurans, is very rare; therefore, dispersal through terrestrial connections is much more likely in this system (Vences *et al.* 2003, Kraus 2015, Fonte *et al.* 2019). This also seems to be in line with the fact that ≥10 other Asterophryinae genera are distributed in these archipelagos (*Austrochaperina* Fry 1912, *Genyophryne* Boulenger 1890, *Barygenys* Parker 1936, *Copiula* Méhely 1901, *Cophixalus* Boettger 1892, *Mantophryne*, *Oreophryne* Boettger 1895, *Paedophryne* Kraus 2010, *Sphenophryne* Peters and Doria 1878, and *Callulops* Boulenger 1888) (Kraus 2021).

Previous phylogenetic relationships among *Hylophorbus* found by Tu *et al.* (2018) and Portik *et al.* (2023) suggested that the genus colonized the BH at least twice, reasonably assuming a non-BH origin of the genus (cf. above). This is also supported by our analyses (Fig. 3), ~7 Mya (node 18) and ~1 Mya (node 32). This scenario is in line with the evolutionary history of *Schefflera* flowering plants and *Exocelina* diving beetles that have also been reported to have dispersed to the BH from the east within similar time frames (Shee *et al.* 2020, Toussaint *et al.* 2021). However, some nodes within clade C and D have only moderate support (nodes 20 and 35), and alternative relationships might lead to distinct biogeographical scenarios. However, all these alternative scenarios imply three independent westward dispersal events towards the BH instead of two (two and one within clade C and D, respectively).

The southern portion of NG, corresponding to the Australian craton, has apparently been colonized secondarily, at least twice, ~6 Mya (node 34) and ~2 Mya (node 41). This highlights the possibility of an early (7–6 Mya) connectivity between the BH and the rest of NG and thus a more important role of the BH in the biotic diversification of NG than currently admitted. This impediment might stem, in part, from the difficulty of sampling the intervening region between the BH and the main part of NG, which correspond to the Bird's Neck, and this has been aptly called 'Zoogeographers' Gap' by Hartert *et al.* (1936).

Finally, we hypothesized that the central range acted as a barrier during the diversification history of *Hylophorbus*. Considering that *Hylophorbus* spp. are lowland to mid-elevation species (≤2300 m a.s.l. according to the current literature; *Hylophorbus richardsi*, Günther 2001), the present-day central range acts unambiguously as an effective barrier, preventing north–south dispersals across NG. This barrier effect is strongly supported in the distributions and phylogenies of many organisms (e.g. Unmack *et al.* 2013, Bruxaux *et al.* 2018, Eldridge *et al.* 2018, Tallowin *et al.* 2018). Our results support this view, given that no major clade occupies both the northern terranes and the Australian craton (Fig. 3), and no dispersal–vicariance events can be recovered from any of our analyses. Nevertheless, the nature of the geographical barrier remains ambiguous, because the timing of the central range uplift is still debated (Hill and Hall 2003, Quarles van Ufford and Cloos 2005), and marine barriers could also have isolated the northern terranes from the putative landmass of the Australian craton (Harrington *et al.* 2017).

CONCLUSION

Focusing on the diversity and biogeography of *Hylophorbus*, a genus of frog endemic to NG, we suggest that its species diversity is 3.5 times higher than currently admitted, that it started to diversify ~9 Mya, and that it subsequently underwent westward dispersals, either from the northern terranes or from the Papuan Peninsula. Moreover, our findings also indicate potential biotic connections between the BH landmass and the rest of NG ~6 Mya. We hypothesize that dispersal following the build-up of terrestrial ecosystems and sea-level variations during the late Miocene explain the extant *Hylophorbus* diversity well. Nevertheless, owing to a lack of sampling in some regions (e.g. western portion and northern foothills of the central range, and Australian craton), our study also highlights that *Hylophorbus* diversity remains known only in part, and therefore so is its history of diversification, a situation that applies to most other NG frog genera.

TAXONOMIC ACCOUNT

Three of the five CCS (see Results, subsection *Integrative consensus*) are named and described below. The specimens are all housed in the Bogor Museum collection [Museum Zoologicum Bogoriense (MZB), Indonesia], and available call recordings are deposited in the 'Sonothèque du Muséum National d'Histoire Naturelle' (https://sonotheque.mnhn.fr/?q=Hylophorbus; Guilbert and Loret 2018; for recording vouchers, see Supporting Information, Table S3). The examined qualitative and quantitative traits are based on the work of Richards and Oliver (2007), Kraus and Allison (2009), and Günther *et al.* (2014). Measurements were taken following a standardized method and terminology (Watters *et al.* 2016), as follows: snout–vent length

(SV); tibia length from the heel to outer surface of flexed knee (TL); horizontal eye diameter (ED); distance from the centre of the naris to the anterior corner of the eye (EN); straight-line distance from the tip of the snout to the anterior corner of the eye (SN); internarinal distance from the centres of both nares (IN); head width at the widest point (HW); head length from the tip of the snout to the posterior margin of tympanum in a straight line (HL); horizontal tympanum diameter (TY); hand length from the proximal edge of the palm to the tip of the third finger (HandL); foot length from the proximal edge of the sole to the tip of the fourth toe (FootL); third finger disc width (3rdF); fourth toe disc width (4thF); first toe length (T1L); and metatarsal tubercle length (MTL). All measurements were made under a binocular stereomicroscope, using digital callipers with a precision of .01 mm, and rounded to .10 mm to avoid pseudo-precision.

Additionally, two other traits were found to be informative: (i) basal subarticular tubercle length (from the most distal to most proximal edge of the tubercle between the proximal phalanges and metacarpal/metatarsal, noted as 1–4sf and 1–5st for finger and toes, respectively), measured on photographs of preserved specimens using the software ImageJ (Schneider *et al.* 2012); and (ii) position of the palmar tubercles on the hand, relative to the palm ('centred' when anterior to the thenar tubercle, or 'proximal' when posterior or laterally aligned with the thenar tubercle). Both characters were found to have diagnostic value when comparing the newly described species (see the species descriptions below; for a schematic representation of the characters and their variation, see Supporting Information, Fig. S10).

Hylophorbus monophonus sp. nov.

(Fig. 4)

Holotype: MZB.Amph.24 348 (field number EAA514), adult male, collected by Antoine Fouquet and Philippe Gaucher, southern slopes of Kumawa Mountains, Bomberai Peninsula, West Papua province, Indonesia (−4.0365, 133.0703; 400 m a.s.l.), 12 November 2014.

Paratypes: One adult male, MZB.Amph.24 346 (EAA510), and two adult females, MZB.Amph.24 347 (EAA511) and MZB. Amph.24 351 (EAA549), collected with the holotype.

Etymology: The specific epithet 'monophonus' is a Latinized masculine compound adjective formed from the Greek adjective 'monos' (alone) and Greek noun 'phone' (sound, voice), as a reference to the single-note calls of this species. The name indicates a character that is diagnostic compared with *Hylophorbus tetraphonus* Günther 2001, a species that displays similar size and colour pattern.

Diagnosis: A *Hylophorbus* species recognizable by the following unique combination of characters: (i) medium size (male SV = 26.0–28.2 mm; female SV = 27.5–27.7 mm); (ii) poorly developed basal subarticular tubercle on T4 and T5 (male 4st = .53–.59 mm; female 4st = .44–.49 mm; male 5st = .52–.66 mm; female 5st = .42–.43 mm); (iii) a thenar tubercle and two palmar tubercles, ovoid, at proximal edge of hand; (iv) absence of lateral stripe (Fig. 4F); (v) dark brown or black lumbar ocellus, with pale orange anterodorsal margin (Fig. 4G); (vi) dark brown pigmentation on anterodorsal flank, forming various shapes, ranging from dark brown irregular blotches to a well-defined 'crescent' shape (Figs 4F, 5A, B); (vii) bright yellow coloration on axilla, groin, and from anterodorsal side of thigh extending to ventral edge of flank (Fig. 4F, G); (viii) overall pale yellow coloration on the ventral surfaces (Fig. 4H); and (ix) single-pulse, single-note calls, with slight frequency modulation and dominant frequency at ~1.3 kHz (Fig. 4D).

Description of the holotype: Adult male (for measurements, see Supporting Information, Table S7). Head as wide as long (HL/HW = .98); nares directed laterally, closer to tip of snout than to eye, internarial distance larger than distance from nostril to anterior edge of eye (EN/IN = .55); snout acute in lateral view, almost truncate in dorsal view. Eye moderately large (EY/SV = .14). Tympanum large (TY/SV = .11, TY/EY = .74), supratympanic fold inconspicuous, outlined in dark brown. Skin finely granular on dorsal surfaces, with sparse flat tubercles, smooth on ventral surfaces. Fingers unwebbed, relative lengths 3 > 4 > 2 > 1, nearly the same for F1, F2, and F4; finger-tips with slightly expanded discs, truncate, all with circum-marginal grooves. Basal subarticular tubercles on F1–F3 more developed (1–3sf = .68–.79 mm) than on F4 (4sf = .60 mm); thenar tubercle and two palmar tubercles present, ovoid, well developed, located at proximal edge of palm, with inner palmar tubercle slightly more anterior. Toes unwebbed, relative lengths 4 > 3 > 5 > 2 > 1; disc almost lacking on T1, slightly expanded on T5, and much larger on T2–T4 (twice width of penultimate phalanges), all with circum-marginal grooves. Subarticular tubercles best developed on T1–T3 (1–3st = .60–.75 mm), basal subarticular tubercles on T4–T5 indistinct; inner metatarsal tubercle ovoid, well developed (MTL = 1.00 mm), others lacking.

Dorsum, suprascapular region, posterodorsal surface of thigh, and dorsal surface of shank light brown, with several scattered small, dark brown blotches; very thin vertebral skin ridge extending from tip of snout to urostyle. Anterior region of flanks with pale grey and dark brown irregular blotches (Fig. 4F), white speckles extending under axilla to anterior abdomen (Fig. 4H). Posterodorsal surface of forelimbs and dorsal surfaces of F3–F4 light reddish brown; brown blotch consistently present between base of F2 and F3; outer side of foot and dorsal surfaces of T4–T5 light reddish brown (Fig. 4F); dorsal surfaces of all fingers and toes with brown blotches. Dorsal and lateral surface of head light reddish brown; dorsal tip of snout, under eye, and margin of naris heavily pigmented with dark brown. Chin, throat, chest, and anterior portion of abdomen mottled with brown and having pale yellow flecks (Fig. 4H). Abdomen, ventral surfaces of thigh, and shank overall pale yellow, fading to translucent skin on anteroventral forelimbs (Fig. 4H). Axilla, groin and anterodorsal thigh to ventral edge of flank bright yellow (Fig. 4G, H). Ventral surface of hands and feet light brown. Pale red blotch above tip of urostyle, margined in black posterolaterally. Iris silver, with dark brown vertical line crossing pupil; pupil margined with incandescent orange.

Variation: Only four specimens are available to assess variation within the sample (Supporting Information, Table S7). Relative size of subarticular tubercles varies between individuals, such

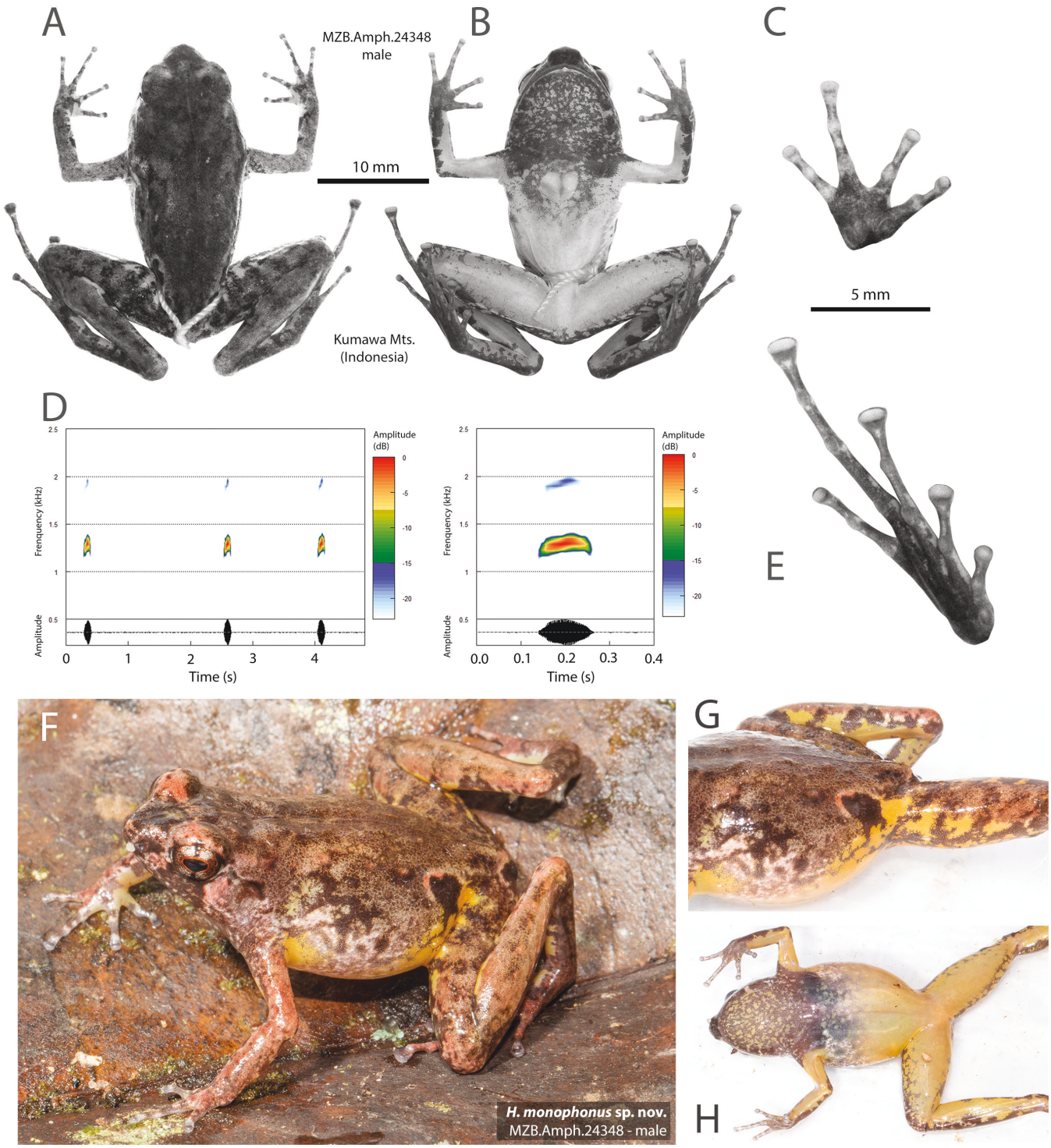

Figure 4. ***Hylophorbus monophonus*** holotype *MZB.Amph.24 348*. A, dorsal view in preservative. B, ventral view in preservative. C, palm of the hand in preservative. D, sonograms and their corresponding oscillograms of a call series and single call (left and right respectively). E, sole of the foot in preservative. F, dorsolateral view in life. G, dorsolateral view of the flank and groin in life. H, ventral view in life. Photographs in preservative by A. Riyanto; photographs in life by A. Fouquet.

that the longest ones on the hand are on F1–F3, and on the foot on T2–T3. The relative position of palmar tubercles is consistent between individuals (proximal; Supporting Information, Fig. S10). Little variation is visible in colour patterns among preserved specimens. The two females exhibit a stronger contrast between dorsal and lateral coloration, in addition to a dark brown 'crescent' shape on the flanks. They also exhibit four well-distinguished dorsal tubercles in the lumbar region, anterior to the lumbar ocellus. Information on colour in life for MZB. Amph.24 351 is not available; therefore, only the colour in life of MZB.Amph.24 346 and MZB.Amph.24 347 is discussed (Fig. 5A, B). Overall, colour pattern as is described for the holotype,

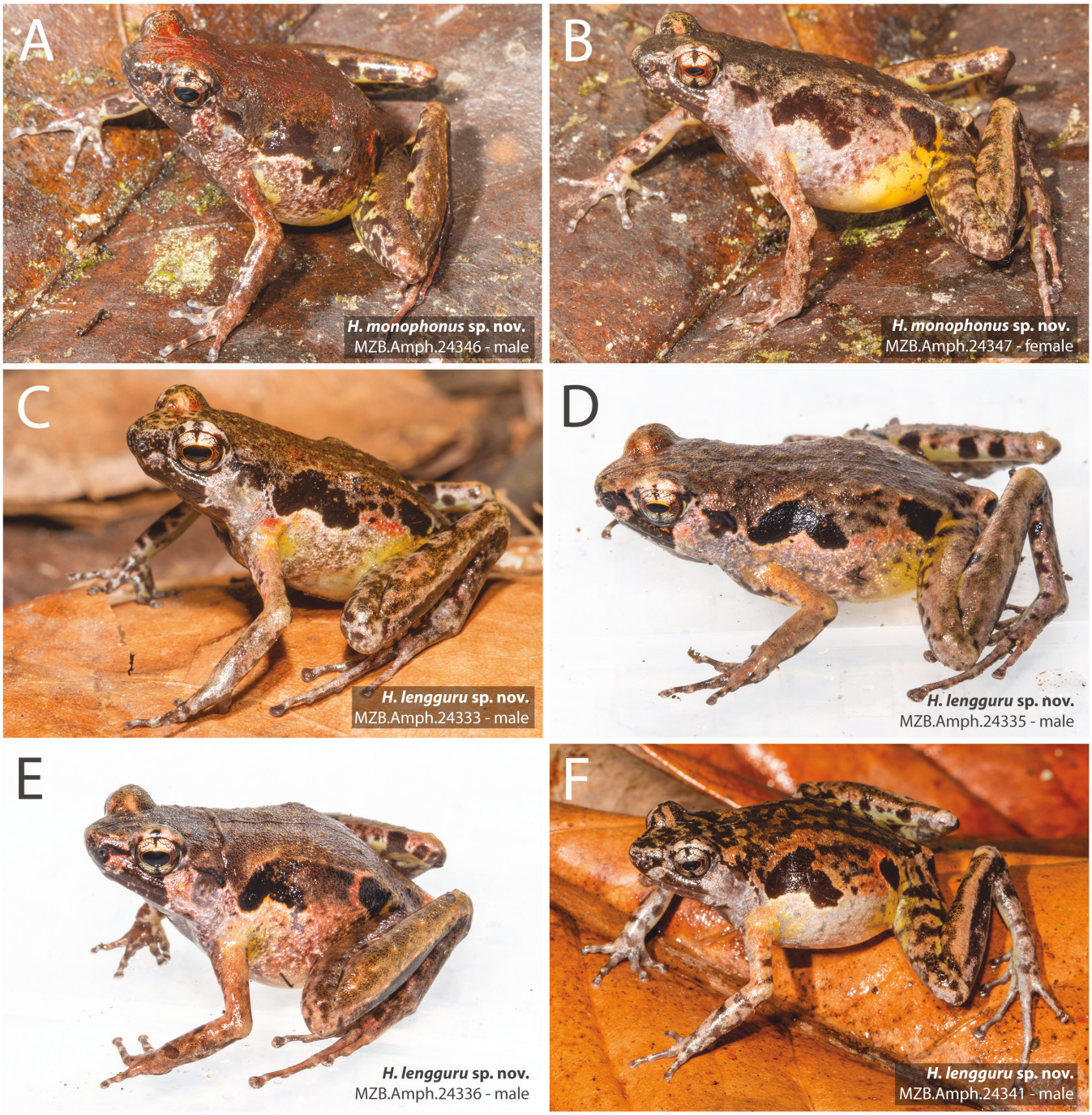

Figure 5. Portraits in life. A, B, ***Hylophorbus monophonus***. A, paratype MZB.Amph.24 346 (male). B, MZB.Amph.24 347 (female). C–F, ***Hylophorbus lengguru***. C, paratype MZB.Amph.24 333 (male). D, MZB.Amph.24 335 (male). E, MZB.Amph.24 336 (male). F, MZB. Amph.24 341 (male). Photographs by A. Fouquet.

with variation observed on the flanks and dorsal coloration. The male MZB.Amph.24 346 dorsum mixes red and dark brown coloration and displays a dark brown blotch with irregular edges on the anterior flank. The female MZB.Amph.24 347 harbours a well-defined dark brown 'crescent' blotch on the anterior flank; the flanks are pale grey (slightly pinkish) from the posterolateral edge of eye to the lumbar ocellus.

Call: We analysed a total of 70 calls from three males (Table 1; Supporting Information, Table S3). The analysed files are deposited in the sound collection of 'La Sonothèque du Muséum National d'Histoire Naturelle' (Supporting Information, Table S3; Guilbert and Loret 2018). The advertisement call consists of a short single note, mean duration 131 ms, range 108–153 ms (Fig. 4D). The dominant frequency is 1.27 kHz (range 1.20–1.32 kHz). Notes can exhibit one harmonic, at a frequency of ~1.90 kHz. Most of the calls (notes) within a call series display similar amplitude and frequency. However, the species sometimes emits a second type of note with two pulses (Supporting Information, Fig. S5C). Mean inter-note duration is 1570 ms (range 635–2395 ms).

Distribution and ecological notes: ***Hylophorbus monophonus*** is known only from the type locality. The species inhabits the leaf litter of pristine lowland rainforest between 300 and 400 m a.s.l. Very little is known about its ecology. Interestingly, specimens of *H. picoides* have been sampled at the same locality (MZB.Amph.24 349 and MZB.Amph.24 350), but not syntopically (1100 m a.s.l.), suggesting that these species might not overlap in their ecology, occupying distinct elevational ranges. Such a pattern of distribution has also been documented in the Wondiwoi Mountains by Günther (2001), where *Hylophorbus wondiwoi* Günther 2001 and *H. tetraphonus* mainly occupy different altitudes.

Comparisons with other species: ***Hylophorbus monophonus*** can be distinguished immediately from *Hylophorbus nigrinus* Günther 2001, *H. picoides* Günther 2001, *H. atrifasciatus*, *H. infulatus*, and *H. sigridae* by the absence of a lateral stripe (Zweifel 1972, Günther 2001, Kraus 2013, Günther *et al.* 2014); from *H. extimus* Zweifel 1972 and *H. myopicus* Zweifel 1972 by smaller body size (26.0–28.2 mm in *H. monophonus* vs. 40.0–49.0 mm); from *H. proekes* Kraus & Allison 2009 and *Hylophorbus sextus* Günther 2001 by its yellow ventral coloration and its single-note calls; and from *H. wondiwoi* by its smaller body size (>32.0 mm in *H. wondiwoi*) and its single-note calls. Colour patterns of *H. tetraphonus* (Bird's Neck species, West Papua, Indonesia), *H. richardsi* (Hela Province, Papua New Guinea), and *Hylophorbus rainerguentheri* Richards & Oliver 2007 (Huon Peninsula, Papua New Guinea) most resemble ***H. monophonus***. However, ***H. monophonus*** is larger (26.0–28.2 mm) than *H. richardsi* (21.3–22.6 mm), its abdomen is yellowish (vs. whitish for *H. richardsi*), and notes are longer (131 ms vs. ~60.5 ms); ***H. monophonus*** has a ventral–lateral and axillary yellow coloration, in addition to a conspicuous dark brown pattern on the flanks, lacking in *H. rainerguentheri*; ***H. monophonus*** has single-note calls, vs. one to five notes in *H. tetraphonus*. Finally, because of the ambiguity surrounding *H. rufescens sensu* Macleay (1878), we cannot compare their morphology explicitly. However, their habitat type differs (lowland rainforest at 300–400 m a.s.l. for ***H. monophonus*** vs. seasonal woodland and mangroves for *H. rufescens*), and their type localities are >1000 km apart, making their conspecificity highly unlikely.

Hylophorbus lengguru sp. nov.

(Fig. 6)

Holotype: MZB.Amph.24 334 (field number EAA304), adult male, collected by Antoine Fouquet and Philippe Gaucher, near Lobo village on Lamansiere Mountain, in the Lengguru foldbelt, Triton Bay, Kaimana Regency, West Papua province, Indonesia (−3.7160, 134.0688; 392 m a.s.l.), 24 October 2014.

Paratopotypes: One adult male, collected at 291 m a.s.l. (MZB.Amph.24 333, EAA281), and three adult males and one female collected with the holotype: MZB.Amph.24 335–7 (EAA305–7; males) and MZB.Amph.24 338 (EAA338; female).

Paratypes: Three adult males and two females collected the 11 November 2014, 40 km southeast of Urisa, in the Lengguru foldbelt, Tuguwara, Kaimana Regency, West Papua province, Indonesia (−3.3653, 133.8382; ~400 m a.s.l.): MZB.Amph.34 341 (EAA457; male), MZB.Amph.24 344 (EAA470; male), 24 345 (EAA475; male), MZB.Amph.24 342 (EAA465; female), and MZB.Amph.24 343 (EAA467; female).

Etymology: The specific epithet is a proper noun in apposition, referring to the collecting localities of the species, all located in the Lengguru foldbelt, and it also refers to the 2014 'Lengguru' expedition, during which the specimens were collected.

Diagnosis: A *Hylophorbus* species recognizable by the following unique combination of characters: (i) medium size (male SV = 24.0–29.0 mm; female SV = 27.3–30.4 mm); (ii) poorly developed, sometimes indistinct, basal subarticular tubercle on T4 and T5 (male 4st = .35–.60 mm; female 4st = .60 mm; male 5st = .49–.59 mm; female 5st = .46 mm); (iii) a thenar tubercle and two palmar tubercles, ovoid, at proximal edge of hand; (iv) absence of lateral stripe (Figs 5C–F, 6F); (v) dark brown or black lumbar ocellus, with reddish anterior margin fading towards a 'crescent'-shaped blackish brown blotch on anterior flank; (vi) yellow and red pigmentation of various intensity around lumbar ocellus and acromial region; (vii) bright yellow groin, axilla, and yellow flecks on rear of thigh; (viii) overall drab whitish yellow coloration on abdomen and ventral surfaces of legs; (ix) well-defined black spot of variable size on superior edge of eye, aligned with vertical dark pigmentation of iris; and (x) calls of one to six single-pulse notes (mean = 3) with an upward frequency modulation (dominant frequency ~1.13 kHz) and up to five harmonics (Fig. 6D).

Description of the holotype: Adult male (for measurements, see Supporting Information, Table S7). Head as wide as long (HL/HW = .98); nares directed laterally, closer to tip of snout than to eye, internarial distance larger than distance from nostril to anterior edge of eye (EN/IN = .63); snout acute in lateral view, rounded in dorsal view, slightly pointed. Eye moderately large (EY/SV = .13). Tympanum large (TY/SV = .08, TY/EY = .65), supratympanic fold inconspicuous, outlined by a black line overlaid by a triangular black–brown coloration, pointing ventrally. Skin finely granular with sparse flat tubercles on dorsal surfaces, smooth on ventral surfaces. Fingers unwebbed, relative lengths 3 > 4 > 2 > 1, nearly the same for F1, F2, and F4; fingers with slightly expanded truncate discs, all with circum-marginal grooves. Subarticular tubercles on all fingers, well developed; thenar tubercle and two palmar tubercles present, ovoid, well developed, at proximal edge of palm, with inner palmar tubercle located slightly more anteriorly. Toes unwebbed, relative lengths 4 > 3 > 5 > 2 > 1; discs on T1 and T5 slightly expanded, ~1.5 times wider than penultimate phalanges, discs much larger on T2–T4, ~3 times wider than penultimate phalanges, all with circum-marginal grooves. Subarticular tubercles mostly developed on T1–T3, basal subarticular tubercles indistinct on T4–T5, inner metatarsal tubercle ovoid, well developed, others lacking.

Posterior dorsum to inter-orbital region brown, anterodorsal head with scattered dark brown spots; very thin vertebral skin ridge extending from tip of snout to urostyle. Ventral half of flank overall pale grey, sharply contrasted with dorsum. Small speckles of black, yellow, grey, and white extend from anterior

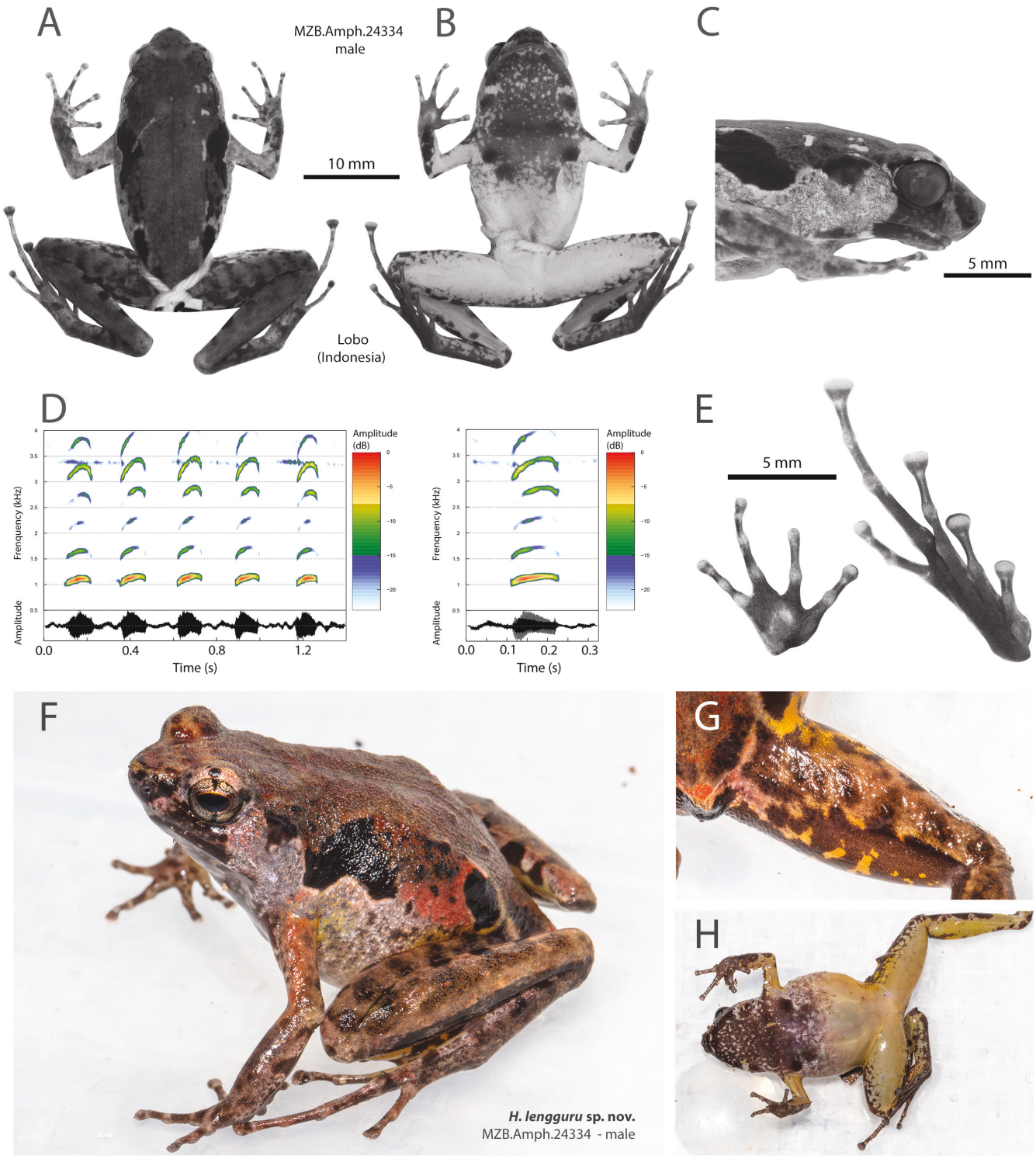

Figure 6. *Hylophorbus lengguru* holotype *MZB.Amph.24 334*. A, dorsal view in preservative. B, ventral view in preservative. C, lateral view in preservative. D, sonograms and their corresponding oscillograms of a call and a single note (left and right, respectively). E, palm of the hand and sole of the foot in preservative. F–H, holotype in life in dorsolateral view (F), dorsal view of the thigh (G), and ventral view (H). Photographs in preservative by A. Riyanto; photographs in life by A. Fouquet.

flank to anterior abdomen. Large anterolateral 'crescent'-shaped blotch and lumbar ocellus both black, middle flank region red, with scattered black spots (Fig. 6F). Posterodorsal forelimb and posteroventral and anterodorsal edge of eye reddish, upper arm with strong red pigmentation; lateral snout and under eye both blackish brown. Chin, throat, chest, and anterior portion of abdomen drab white heavily mottled with brown, with scattered light grey flecks; distinct dark brown blotch on each side of posterior submandibular region (Fig. 6B, H). Anteroventral forelimbs, axilla, abdomen, and ventral thigh greyish yellow,

almost transparent. Ventral shank, groin, and flecks on posterior dorsal thigh bright yellow. Hands and feet reddish brown, with dark brown blotches. Ventral surface of hands and feet light brown. Red blotch above tip of urostyle, margined in black posterolaterally. Iris silver, with dark brown vertical line crossing pupil; pupil margined with bright orange.

Variation: Eleven specimens are available to assess variation within the samples (Supporting Information, Table S7). The longest basal subarticular tubercle on the hand is either 1sf or 2sf, and always 2st on the foot. There is extensive variation in the relative size of 3st (3st/SV = .40–.60; male 3st = .61–.79 mm) compared with the other basal subarticular tubercles, and 4st and 5st are either indistinct or at least less developed than other tubercles (Supporting Information, Fig. S6B). The relative size and shape of the palmar tubercles varies greatly between specimens (e.g. palmar tubercles seemingly fused on MZB. Amph.24 341 and MZB.Amph.24 342; palmar tubercles thin and elongated on MZB.Amph.24 333 and MZB.Amph.24 335), but their positioning relative to the palm remains the same (proximal; Supporting Information, Fig. S10). Dorsal and lateral colour patterns of preserved specimens are remarkably similar, except for paratype MZB.Amph.24 241, which displays striking blackish-brown 'wavy' stripes on the dorsum, top of head, and top of thigh (Fig. 5F). Mottling on the chin and throat varies in density between all specimens, such that it is nearly solid dark brown with very few unpigmented areas on MZB.Amph.24 333 and MZB.Amph.24 345. Nevertheless, the dark brown blotch on both sides of the posterior submandibular region is still distinguishable. Information on colour in life is available only for MZB.Amph.24 333, MZB.Amph.24 335, MZB.Amph.24 336, and MZB.Amph.24 341; only those are discussed (Fig. 5C–F). Overall, the colour pattern in life is as described for the holotype, with the exception of MZB.Amph.24 341, which displays striking blackish-brown motifs in dorsal view, as discussed above. Variation in pigmentation intensity in the margin of the lumbar ocellus and acromial region is observed between all specimens.

Call: We analysed a total of 53 calls from two males, one from each locality (Table 1; Supporting Information, Table S3). The analysed files are deposited in the sound collection of 'La Sonothèque du Muséum National d'Histoire Naturelle' (Supporting Information, Table S3; Guilbert and Loret 2018). The advertisement call consists of one to six single-pulse notes (mean = 3), and mean note duration is 107 ms (range 89.0–138 ms) (Table 1; Fig. 6D). Mean inter-note duration is 163 ms (range 132–208 ms). Mean dominant frequency is 1.13 kHz (range 1.10–1.14 kHz). Notes can exhibit up to five harmonics, between 1.5 and 3.5 kHz (Fig. 6D; Supporting Information, Fig. S5D). Notes within a call are remarkably similar in their durations, frequency, and amplitude modulations (Table 1). Frequency modulation never exceeds an increase of .20 kHz.

Distribution and ecological notes: ***Hylophorbus lengguru*** is known from Lobo and Tuguwara, both in the Lengguru foldbelt (West Papua province, Indonesia). The species inhabits the leaf litter of pristine lowland rainforest between 300 and 400 m a.s.l.

Comparisons with other species: ***Hylophorbus lengguru*** can be distinguished immediately from *H. nigrinus, H. picoides, H. atrifasciatus, H. infulatus*, and *H. sigridae* by the absence of a lateral stripe; from *H. extimus* and *H. myopicus* by its smaller size (23.9–30.4 mm in *H. lengguru* vs. 40.0–49.0 mm). It can be distinguished from *H. proekes* and *H. sextus* by its greyish-yellow ventral coloration and its single-pulsed notes. It is further distinguished from *H. richardsi* by its yellowish ventral coloration; from *H. rainerguentheri* by its greyish flanks and the presence of a lateral 'crescent'-shaped blotch; and from ***H. monophonus*** by the absence of a bright yellow coloration on the posteroventral flanks. ***Hylophorbus lengguru*** is also distinguished from *H. richardsi*, *H. rainerguentheri*, and ***H. monophonus*** by having multi-note calls. ***Hylophorbus lengguru*** can be distinguished from *H. wondiwoi* by its light-brown flanks more contrasting with the dorsum, and by its notes being twice as long (100 ms for ***H. lengguru*** vs. ~50 ms). Colour patterns of ***H. lengguru*** resemble those of *H. tetraphonus* (Bird's Neck species, West Papua province, Indonesia), but it can be distinguished by its call: ***H. lengguru*** notes are lower (dominant frequency 1.13 kHz vs. ~1.75 kHz) and have lower frequency modulation, reaching an increase of <.20 kHz (vs. .50 kHz). Finally, because of the ambiguity surrounding *H. rufescens sensu* Macleay (1878), we cannot compare their morphology explicitly. However, their habitat type differs (lowland rainforest at 300–400 m a.s.l. for ***H. lengguru*** vs. seasonal woodland and mangroves for *H. rufescens*), and their type localities are >1000 km apart, making their conspecificity highly unlikely.

Hylophorbus maculatus sp. nov.

(Fig. 7)

Holotype: MZB.Amph.24 339 (field number EAA357), adult male, collected by Antoine Fouquet and Philippe Gaucher, near Lobo village on Lamansiere Mountain, in the Lengguru foldbelt, Triton Bay, Kaimana Regency, West Papua province, Indonesia (−3.7291, 134.0617; 1021 m a.s.l.), 27 October 2014.

Paratypes: One adult male, MZB.Amph.24 340 (EAA358), collected with the holotype.

Etymology: The specific epithet is a Latin masculine adjective meaning 'speckled' or 'spotted', in reference to the overall spotted pattern on the ventral surfaces and flanks of this species.

Diagnosis: A *Hylophorbus* species recognizable by the following unique combination of characters: (i) small size (male SV = 23.4–24.2 mm, mean = 23.8 mm); (ii) strongly developed basal subarticular tubercle on F3–F4 (male 3sf = .80–.82 mm; male 4sf = .77–.83 mm), T3 (male 3st = .70–.92 mm), and T4 (male 4st = .81–.92 mm) (Supporting Information, Fig. S6B); (iii) a thenar tubercle and two palmar tubercles, inner palmar tubercle at centre of palm; (iv) short, dark brown lateral stripe extending from the posterolateral edge of the eye to middle region of the flank (Fig. 7E, G); (v) dark brown lumbar ocellus; (vi) yellow groin; (vii) overall whitish ground coloration on ventral surfaces; (viii) discontinuous dark line extending from dorsal edge of lumbar ocellus to posterior lateral edge of eye, above short lateral stripe (Fig. 7E, G); (ix) conspicuous dark blotches on the posterior dorsal thighs and flank between short lateral stripe and lumbar ocellus; and (x) dark brown mottling on the ventral thighs, medial feet, and anterior abdomen.

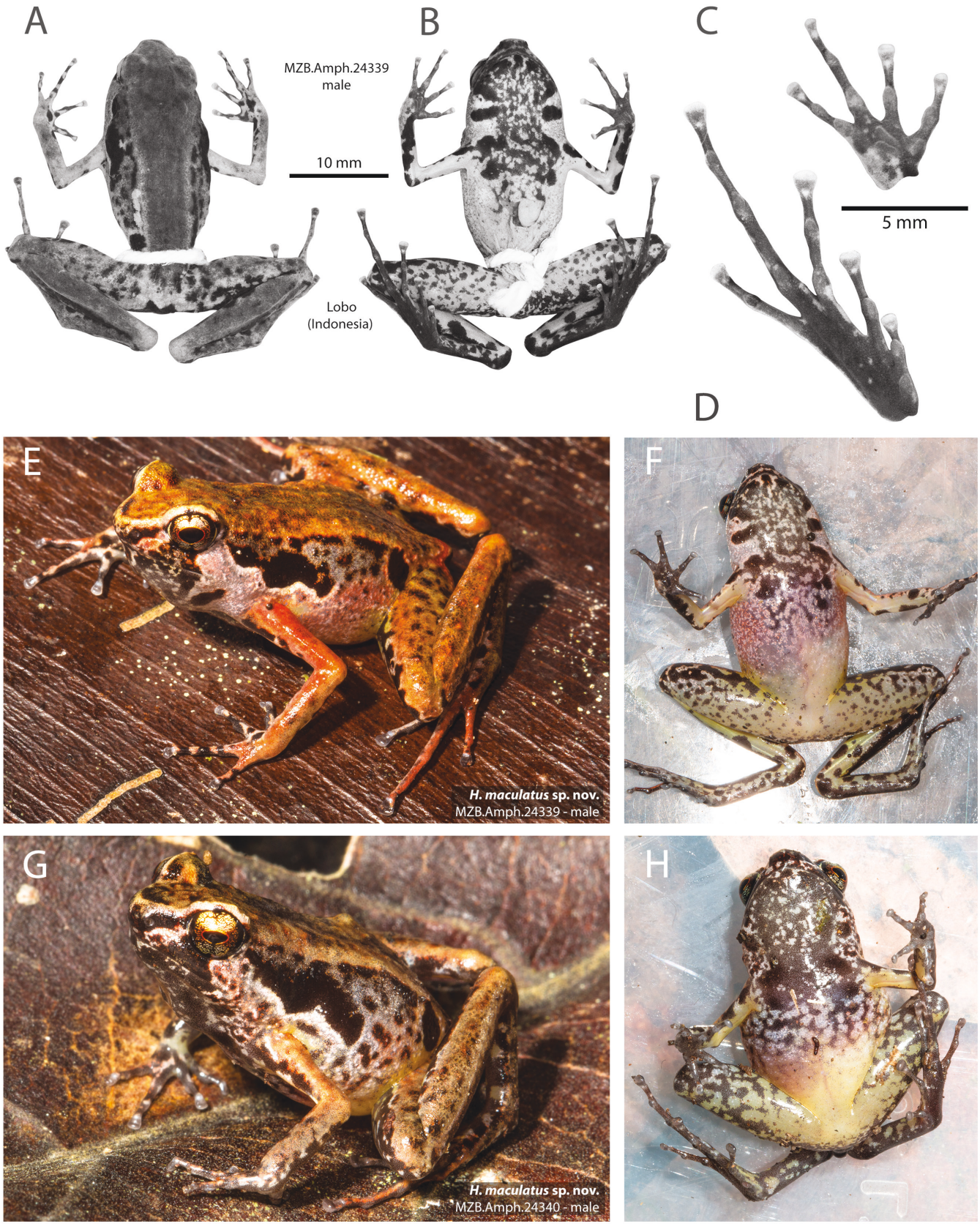

Figure 7. ***Hylophorbus maculatus*** holotype *MZB.Amph.24 339*. A, dorsal view in preservative. B, ventral view in preservative. C, palm of the hand in preservative. D, sole of the foot in preservative. E, F, holotype in life in dorsolateral view (E) and ventral view (F). G, H, paratype MZB.Amph.24 340 in life in dorsolateral view (G) and ventral view (H). Photographs in preservative by A. Riyanto; photographs in life by A. Fouquet.

Description of the holotype: Adult male (for measurements, see Supporting Information, Table S7). Head slightly longer than wide (HL/HW = 1.15); nares directed laterally, closer to tip of snout than to eye, internarial distance larger than distance from nostril to anterior edge of eye (EN/IN = .84); snout acute in lateral view, truncate in dorsal view. Eye moderately large (EY/SV = .14). Tympanum large (TY/SV = .08, TY/EY = .58), supratympanic fold inconspicuous. Skin slightly granular on all dorsal surfaces, with several small tubercles on dorsum, finely granular on ventral surfaces. Fingers unwebbed, relative lengths 3 > 2 > 1 > 4; tips with slightly expanded truncate discs, all with circum-marginal grooves. Subarticular tubercles on all fingers, well developed; thenar tubercle well developed, ovoid; palmar tubercles more elongated; inner palmar tubercle at centre of palm. Toes unwebbed, relative lengths 4 > 3 > 5 > 2 > 1; discs on T1 and T5 slightly expanded, ~1.5 times wider than penultimate phalanges, discs larger on T2–T4, ~2 times wider than penultimate phalanges, all with circum-marginal grooves. Subarticular tubercles well developed on T1–T4, especially on T3 (3st = .92 mm), basal subarticular tubercles poorly developed on T5 (5st = .51 mm), inner metatarsal tubercle ovoid, well developed (MTL = 1.55 mm), others lacking.

Dorsum from head to shanks yellowish brown, with scattered brown spots on suprascapular region and top of thighs (Fig. 7E). Lumbar ocellus dark brown, margined posteroventrally with bright yellow; groin bright yellow. Flank overall reddish grey, separated from dorsum by one discontinuous dark brown line extending from dorsal edge of lumbar ocellus to posteriolateral edge of eye. Small red, white, and brown speckles from anterior flank to anterior abdomen. Short black lateral stripe running from anterior edge of tympanum (which it overlays) to middle of flank, margined ventrally with white, separated from lumbar ocellus by grey coloration containing small black blotches (Fig. 7E). Dorsal surfaces of F3–F4, lateral surfaces of feet, dorsal T4–T5, and posterodorsal surfaces of forelimb red (more intense on upper arm). Dorsally, F1–F2 and T1–T3 grey, with dark brown irregular spots on all fingers; dark brown blotch between base of F2 and F3; ventral surface of hands and feet brown. Chin, throat, chest, and anterior half of abdomen with inconsistent dark brown mottling; distinct dark brown blotch on each side of posterior submandibular region (Fig. 7F, H). Ventral surfaces overall whitish (Fig. 7F), ventral surfaces of legs with dark brown mottling. Red pigmentation above tip of urostyle, margined in black posterolaterally. Black colour around naris and eye in contact. Iris golden–copper, with dark brown vertical line crossing pupil; pupil margined with bright orange.

Variation: Assessment of variation is based on only two specimens (Supporting Information, Table S7). Longest basal subarticular tubercle on the hand either 2sf or 4sf, and 3st or 4st on the foot. Mostly, variation in the size of the 3st (3st/SV = .05 and .07; 3st = .70 and .92 mm) (Supporting Information, Fig. S6B). The shape of the palmar tubercles varies between specimens (rounder on MZB.Amph.24 340), but their positioning relative to the palm remains the same (centred; Supporting Information, Fig. S10). Colour pattern in life or in preservative of the two available specimens is similar, with the exception of the chin and throat mottling, which are pronounced and consistent in the paratype (MZB.Amph.24 340), and the dorsal colour is light brown in the paratype vs. yellowish brown in the holotype. The red pigmentation on the upper arm and hand of the paratype is also less conspicuous than on the holotype, but it remains conspicuous on the foot.

Call: Unknown.

Distribution and ecological notes: ***Hylophorbus maculatus*** is known only from the type locality, a pristine lower montane forest at ~1000 m a.s.l. Interestingly, specimens of ***H. lengguru*** have been sampled in the same locality (specimens MZB. Amph.24 333–8), but non-syntopically (occurring at 300–400 m a.s.l.), suggesting that these species might not overlap in their ecologies and along the elevation gradient, as discussed above.

Comparisons with other species: ***Hylophorbus maculatus*** can be distinguished immediately from *H. rainerguentheri*, *H. richardsi*, *H. sextus*, *H. tetraphonus*, *H. wondiwoi*, *H. proekes*, *H. infulatus*, *H. atrifasciatus*, *H. nigrinus*, ***H. monophonus***, and ***H. lengguru*** by the presence of a short lateral stripe (extending from the posterolateral edge of the eye to the middle region of the flank); and from *H. extimus* and *H. myopicus* by its much smaller size (23.4–24.2 mm in ***H. maculatus*** vs. 40.0–49.0 mm). ***Hylophorbus maculatus*** resembles *H. picoides* and *H. sigridae*, which also exhibit a short lateral stripe, but can be distinguished from them by the presence of a black line extending from the dorsal edge of the lumbar ocellus to the eye, and by the presence of dark brown blotches on the flank, between the posterior end of the short lateral stripe and the lumbar ocellus. Finally, because of the ambiguity surrounding *H. rufescens sensu* Macleay (1878), we cannot compare their morphology explicitly. However, their habitat type differs (lower montane rainforest at ~1000 m a.s.l. for ***H. maculatus*** vs. seasonal woodland and mangroves for *H. rufescens*), and their type localities are >1000 km apart, making their conspecificity highly unlikely.

SUPPLEMENTARY DATA

Supplementary data is available at *Zoological Journal of the Linnean Society* online.

ACKNOWLEDGEMENTS

We are thankful to Molly Hagemann, who managed the loan procedures of the *Hylophorbus* materials deposited in the Bernice Pauahi Bishop Museum (BPBM), and to Frank Tillack, who managed the loan procedures of the materials deposited in the Berlin Museum of Natural History (ZMB). The data generated were extremely valuable to the achievement of this project. We are particularly grateful to Laurent Pouyaud, Gono Semiadi, Régis Hocdé, Jacques Slembrouck, and Kadarusman, who organized the *Lengguru* expedition in 2014. Furthermore, our field work in the Lengguru area and in the Kumawa Mountains could not have proceeded without the hospitality and partnership of the villagers of Lobo and Nusa Ulan, who provided excellent guidance and assistance during the 2014 field trips. Finally, we are grateful to the reviewers and the Associate Editor for their valuable remarks and suggestions, these greatly improved previous versions of this manuscript.

AUTHOR CONTRIBUTIONS

Flavien Ferreira (Data curation, Formal analysis, Visualization, Writing—original draft & editing), Antoine Fouquet (Data curation

& collection, Methodology, Project administration, Writing—review & editing), Fred Kraus (Data curation & collection, Writing—review & editing), Stephen Richards (Data curation & collection, Writing—review & editing), Rainer Günther (Data curation & collection, Writing—review & editing), Paul Oliver (Writing—review & editing), Christophe Thébaud (Data collection, Writing—review & editing), Wahyu Trilaksono (Data collection, Writing—review), Evy Ayu Arida (Data collection, Writing—review), Amir Hamidy (Data curation, Writing—review), Awal Riyanto (Data collection, Writing—review), Philippe Gaucher (Data collection, Writing—review), and Burhan Tjaturadi (Data collection, Writing—review).

CONFLICT OF INTEREST:

None declared.

FUNDING

The first author was supported by the Ministère de l'Enseignement Supérieur et de la Recherche PhD scholarship throuh SEVAB graduate school. Fieldwork in Lengguru was conducted under the RISTEK research permit number 304/SIP/FRP/SM/X/2014, supported by the Lengguru Project (www.lengguru.org) conducted by the French Institut de Recherche pour le Développement (IRD), the Indonesian Institute of Sciences (LIPI), with the Research Center for Biology (RCB) and the Research Center for Oceanography (RCO), the University of Papua (UNIPA), the University of Cendrawasih (UNCEN), the University of Musamus (UNMUS), and the Polytechnic KP Sorong, with corporate sponsorship from COLAS and TIPCO groups, Veolia Water, and the Total Foundation, and assistance from the Institut Français in Indonesia (IFI) and the French embassy in Jakarta. Fieldwork leading to *Hylophorbus* materials deposited in BPBM was supported by National Science Foundation grants DEB-0103794, DEB-0743890, and DEB-1145453.

DATA AVAILABILITY

Data used in the analyses have been deposited in online repositories: GenBank (molecular data; for accession numbers, see Supporting Information, Table S1), OSF (mtDNA and nu + mtDNA datasets; https: //doi.org/10.17605/OSF.IO/XVJQU), and in the 'Sonothèque du Muséum National d'histoire Naturelle' (acoustic data; https://sonotheque.mnhn.fr/?q=Hylophorbus); or are available directly in the Supporting Information.

REFERENCES

Arida E, Ashari H, Dahruddin H *et al*. Exploring the vertebrate fauna of the Bird's Head Peninsula (Indonesia, West Papua) through DNA barcodes. *Molecular Ecology Resources* 2021;**21**:2369–87.

Audacity Team. 2022. *Audacity(R): free audio editor and recorder [computer application]*.

Bailly V, Pubellier M, Ringenbach JC *et al*. Deformation zone 'jumps' in a young convergent setting; the Lengguru fold-and-thrust belt, New Guinea Island. *Lithos* 2009;**113**:306–17. https://doi.org/10.1016/j.lithos.2009.08.013

Baldwin SL, Fitzgerald PG, Webb LE. Tectonics of the new Guinea region. *Annual Review of Earth and Planetary Sciences* 2012;**40**:495–520. https://doi.org/10.1146/annurev-earth-040809-152540

Bandelt HJ, Forster P, Röhl A. Median-joining networks for inferring intraspecific phylogenies. *Molecular Biology and Evolution* 1999;**16**:37–48. https://doi.org/10.1093/oxfordjournals.molbev.a026036

Beehler BM, Laman T. *Nature and Culture of Earth's Grandest Island*. Hope GS (ed.). Princeton: Princeton University Press, 2020.

Bouckaert R, Heled J, Kühnert D *et al*. BEAST 2: a software platform for Bayesian evolutionary analysis. *PLoS Computational Biology* 2014;**10**:e1003537.

Brito D. Overcoming the Linnean shortfall: data deficiency and biological survey priorities. *Basic and Applied Ecology* 2010;**11**:709–13. https://doi.org/10.1016/j.baae.2010.09.007

Bruxaux J, Gabrielli M, Ashari H *et al*. Recovering the evolutionary history of crowned pigeons (Columbidae: *Goura*): implications for the biogeography and conservation of New Guinean lowland birds. *Molecular Phylogenetics and Evolution* 2018;**120**:248–58. https://doi.org/10.1016/j.ympev.2017.11.022

Cámara-Leret R, Frodin DG, Adema F *et al*. New Guinea has the world's richest island flora. *Nature* 2020;**584**:579–83. https://doi.org/10.1038/s41586-020-2549-5

Ceballos G, Ehrlich PR, Dirzo R. Biological annihilation via the ongoing sixth mass extinction signaled by vertebrate population losses and declines. *Proceedings of the National Academy of Sciences of the United States of America* 2017;**114**:E6089–96. https://doi.org/10.1073/pnas.1704949114

Ceballos G, Ehrlich PR, Raven PH. Vertebrates on the brink as indicators of biological annihilation and the sixth mass extinction. *Proceedings of the National Academy of Sciences of the United States of America* 2020;**117**:13596–602. https://doi.org/10.1073/pnas.1922686117

Chernomor O, von Haeseler A, Minh BQ. Terrace aware data structure for phylogenomic inference from supermatrices. *Systematic Biology* 2016;**65**:997–1008. https://doi.org/10.1093/sysbio/syw037

Davies HL. The geology of New Guinea - the cordilleran margin of the Australian continent. *Episodes* 2012;**35**:87–102. https://doi.org/10.18814/epiiugs/2012/v35i1/008

Dayrat B. Towards integrative taxonomy. *Biological Journal of the Linnean Society* 2005;**85**:407–15. https://doi.org/10.1111/j.1095-8312.2005.00503.x

de Queiroz K. Species concepts and species delimitation. *Systematic Biology* 2007;**56**:879–86. https://doi.org/10.1080/10635150701701083

di Marco M, Chapman S, Althor G *et al*. Changing trends and persisting biases in three decades of conservation science. *Global Ecology and Conservation* 2017;**10**:32–42.

Dinerstein E, Wikramanayake ED. Beyond 'hotspots': how to prioritize investments to conserve biodiversity in the Indo-Pacific region. *Conservation Biology* 1993;**7**:53–65. https://doi.org/10.1046/j.1523-1739.1993.07010053.x

Drummond AJ, Rambaut A. BEAST: Bayesian evolutionary analysis by sampling trees. *BMC Evolutionary Biology* 2007;**7**:214. https://doi.org/10.1186/1471-2148-7-214

Duellman WE, Borkin LJ, Campbell JA, *et al*. *Patterns of Distribution of Amphibians. A Global Perspective,* Duellman WE (ed.). Baltimore: The Johns Hopkins University Press, 1999.

Eldridge MDB, Potter S, Helgen KM *et al*. Phylogenetic analysis of the tree-kangaroos (*Dendrolagus*) reveals multiple divergent lineages within New Guinea. *Molecular Phylogenetics and Evolution* 2018;**127**:589–99. https://doi.org/10.1016/j.ympev.2018.05.030

Feng YJ, Blackburn DC, Liang D *et al*. Phylogenomics reveals rapid, simultaneous diversification of three major clades of Gondwanan frogs at the Cretaceous–Paleogene boundary. *Proceedings of the National Academy of Sciences of the United States of America* 2017;**114**:E5864–70.

Fonte LFM, Mayer M, Lötters S. Long-distance dispersal in amphibians. *Frontiers of Biogeography* 2019;**11**:e44577.

Fouquet A, Gilles A, Vences M *et al*. Underestimation of species richness in Neotropical frogs revealed by mtDNA analyses. *PLoS One* 2007;**2**:e1109. https://doi.org/10.1371/journal.pone.0001109

Fouquet A, Cassini CS, Haddad CFB *et al*. Species delimitation, patterns of diversification and historical biogeography of the Neotropical frog genus *Adenomera* (Anura, Leptodactylidae). *Journal of Biogeography* 2014;**41**:855–70.

Fouquet A, Leblanc K, Framit M *et al*. Species diversity and biogeography of an ancient frog clade from the Guiana Shield (Anura: Microhylidae: *Adelastes, Otophryne, Synapturanus*) exhibiting spectacular phenotypic diversification. *Biological Journal of the Linnean Society* 2021;**132**:233–56. https://doi.org/10.1093/biolinnean/blaa204

Fouquet A, Cornuault J, Rodrigues MT *et al*. Diversity, biogeography, and reproductive evolution in the genus *Pipa* (Amphibia: Anura: Pipidae). *Molecular Phylogenetics and Evolution* 2022;**170**. https://doi.org/10.1016/j.ympev.2022.107442

Frost DR. Amphibian Species of the World: an Online Reference. *Amphibian Species of the World*. 2023. Last accessed on July 2023. https://amphibiansoftheworld.amnh.org

Georges A, Zhang X, Unmack P, Reid BN, Le M, McCord WP. Contemporary genetic structure of an endemic freshwater turtle reflects Miocene orogenesis of New Guinea. *Biological Journal of the Linnean Society* 2014; **111**:192–208. https://doi.org/10.1111/bij.12176

Giam X, Scheffers BR, Sodhi NS *et al*. Reservoirs of richness: least disturbed tropical forests are centres of undescribed species diversity. *Proceedings of the Royal Society B: Biological Sciences* 2012;**279**:67–76. https://doi.org/10.1098/rspb.2011.0433

Gold DP, White LT, Gunawan I *et al*. Relative sea-level change in western New Guinea recorded by regional biostratigraphic data. *Marine and Petroleum Geology* 2017;**86**:1133–58. https://doi.org/10.1016/j.marpetgeo.2017.07.016

Guilbert F, Loret P. La sonothèque du Muséum National d'Histoire Naturelle. 2018. Last accessed on 6 January 2023. https://sonotheque.mnhn.fr/?q=&tbs=qr:nv,qr:e

Günther R. The Papuan frog genus *Hylophorbus* (Anura: Microhylidae) is not monospecific: description of six new species. *Russian Journal of Herpetology* 2001;**8**:81–104.

Günther R, Richards SJ, Dahl C. Nine new species of microhylid frogs from the Muller Range in western Papua New Guinea (Anura, Microhylidae). *Vertebrate Zoology* 2014;**64**:59–94. https://doi.org/10.3897/vz.64.e31463

Hall R. The plate tectonics of Cenozoic SE Asia and the distribution of land and sea. In: Hall R, Holloway JD (eds.), *Biogeography and Geological Evolution of SE Asia*. Zeeland: Backhuys, 1998, 99–131.

Hall R. Cenozoic geological and plate tectonic evolution of SE Asia and the SW Pacific: computer-based reconstructions, model and animations. *Journal of Asian Earth Sciences* 2002;**20**:353–431. https://doi.org/10.1016/s1367-9120(01)00069-4

Hall R. Southeast Asia's changing palaeogeography. *Blumea - Biodiversity, Evolution and Biogeography of Plants* 2009;**54**:148–61. https://doi.org/10.3767/000651909x475941

Hall R. Late Jurassic–Cenozoic reconstructions of the Indonesian region and the Indian Ocean. *Tectonophysics* 2012;**570–571**:1–41. https://doi.org/10.1016/j.tecto.2012.04.021

Harrington L, Zahirovic S, Flament N *et al*. The role of deep Earth dynamics in driving the flooding and emergence of New Guinea since the Jurassic. *Earth and Planetary Science Letters* 2017;**479**:273–83. https://doi.org/10.1016/j.epsl.2017.09.039

Hartert E, Paludan K, Rothschild W *et al*. Ornithologische Ergebnisse der Expedition Stein 1931–1932 IV Die Vogel des Weyland-Gebirges und seines Vorlandes. *Mitteilungen aus dem Zoologischen Museum in Berlin* 1936;**21**:11–240.

Hill EC, Fraser CJ, Gao DF *et al*. Resolving the deep phylogeny: implications for early adaptive radiation, cryptic, and present-day ecological diversity of Papuan microhylid frogs. *Molecular Phylogenetics and Evolution* 2022;**177**:107618. https://doi.org/10.1016/j.ympev.2022.107618

Hill EC, Gao DF, Polhemus DA *et al*. Testing geology with biology: plate tectonics and the diversification of microhylid frogs in the Papuan region. *Integrative Organismal Biology* 2023;**5**:obad028. https://doi.org/10.1093/iob/obad028

Hill KC, Hall R. Mesozoic-Cenozoic evolution of Australia's New Guinea margin in a west Pacific context. *Evolution and Dynamics of the Australian Plate*. Boulder: Geological Society of America, pp. 259–293; 2003.

Hime PM, Lemmon AR, Lemmon ECM *et al*. Phylogenomics reveals ancient gene tree discordance in the amphibian tree of life. *Systematic Biology* 2021;**70**:49–66.

Hortal J, de Bello F, Diniz-Filho JAF *et al*. Seven shortfalls that beset large-scale knowledge of biodiversity. *Annual Review of Ecology, Evolution, and Systematics* 2015;**46**:523–49. https://doi.org/10.1146/annurev-ecolsys-112414-054400

Jongsma GFM, Barej MF, Barratt CD *et al*. Diversity and biogeography of frogs in the genus *Amnirana* (Anura: Ranidae) across sub-Saharan Africa. *Molecular Phylogenetics and Evolution* 2018;**120**:274–85. https://doi.org/10.1016/j.ympev.2017.12.006

Kalyaanamoorthy S, Minh BQ, Wong TKF *et al*. ModelFinder: fast model selection for accurate phylogenetic estimates. *Nature Methods* 2017;**14**:587–9. https://doi.org/10.1038/nmeth.4285

Kassambara A, Mundt F. *Factoextra: Extract and Visualize the Results of Multivariate Data Analyses. R Package*. 2020. Last accessed on March 2022. https://CRAN.R-project.org/package=factoextra

Katoh K, Rozewicki J, Yamada KD. MAFFT online service: multiple sequence alignment, interactive sequence choice and visualization. *Briefings in Bioinformatics* 2019;**20**:1160–6. https://doi.org/10.1093/bib/bbx108

Kennedy JD, Marki PZ, Reeve AH *et al*. Diversification and community assembly of the world's largest tropical island. *Global Ecology and Biogeography* 2022;**31**:1078–89. https://doi.org/10.1111/geb.13484

Köhler F, Günther R. The radiation of microhylid frogs (Amphibia: Anura) on New Guinea: a mitochondrial phylogeny reveals parallel evolution of morphological and life history traits and disproves the current morphology-based classification. *Molecular Phylogenetics and Evolution* 2008;**47**:353–65. https://doi.org/10.1016/j.ympev.2007.11.032

Köhler J, Jansen M, Rodríguez A *et al*. The use of bioacoustics in anuran taxonomy: theory, terminology, methods and recommendations for best practice. *Zootaxa* 2017;**4251**:1–124. https://doi.org/10.11646/zootaxa.4251.1.1

Kraus F. A new species of *Hylophorbus* (Anura: Microhylidae) from Papua New Guinea. *Current Herpetology; Kyoto* 2013;**32**:102–11.

Kraus F. A new species of the miniaturized frog genus *Paedophryne* (Anura: Microhylidae) from Papua New Guinea. *Occasional Papers of the University of Michigan Museum of Zoology* 2015;**745**:1–11.

Kraus F. A herpetofauna with dramatic endemism signals an overlooked biodiversity hotspot. *Biodiversity and Conservation* 2021;**30**:3167–83. https://doi.org/10.1007/s10531-021-02242-3

Kraus F, Allison A. New species of frogs from Papua New Guinea. *Bishop Museum Occasional Papers* 2009;**104**:1–36.

Landis MJ, Matzke NJ, Moore BR *et al*. Bayesian analysis of biogeography when the number of areas is large. *Systematic Biology* 2013;**62**:789–804. https://doi.org/10.1093/sysbio/syt040

Leaché AD, Koo MS, Spencer CL *et al*. Quantifying ecological, morphological, and genetic variation to delimit species in the coast horned lizard species complex (*Phrynosoma*). *Proceedings of the National Academy of Sciences of the United States of America* 2009;**106**:12418–23.

Leigh JW, Bryant D. POPART: full-feature software for haplotype network construction. *Methods in Ecology and Evolution* 2015;**6**:1110–6. https://doi.org/10.1111/2041-210x.12410

Macleay W. The batrachians of the 'Chevert' Expedition. *Proceedings of the Linnean Society of New South Wales* 1878;**2**:135–8.

Marki PZ, Jønsson KA, Irestedt M *et al*. Supermatrix phylogeny and biogeography of the Australasian Meliphagides radiation (Aves: Passeriformes). *Molecular Phylogenetics and Evolution* 2017;**107**:516–29. https://doi.org/10.1016/j.ympev.2016.12.021

Marshall AJ, Beehler BM. *Ecology of Indonesian Papua Part One*. Hong Kong: Periplus Eds. 2007.

Matzke NJ. *BioGeoBEARS: BioGeography with Bayesian (and likelihood) Evolutionary Analysis with R Scripts*. 2018. Last accessed on June 2023. https://github.com/nmatzke/BioGeoBEARS

Matzke NJ. Statistical comparison of DEC and DEC+J is identical to comparison of two ClaSSE submodels, and is therefore valid. *Journal of Biogeography* 2021;**49**:1805–24. https://doi.org/10.1111/jbi.14346

McDonald PJ, Brown RM, Kraus F *et al*. Cryptic extinction risk in a western Pacific lizard radiation. *Biodiversity and Conservation* 2022;**31**:2045–62.

Milá B, Bruxaux J, Friis G *et al*. A new, undescribed species of *Melanocharis* berrypecker from western New Guinea and the evolutionary history of the family Melanocharitidae. *Ibis* 2021;**163**:1310–29. https://doi.org/10.1111/ibi.12981

Miller KG, Browning J, Schmelz WJ *et al.* Cenozoic sea-level and cryospheric evolution from deep-sea geochemical and continental margin records. *Science Advances* 2020;**6**:eaaz1346. https://doi.org/10.1126/sciadv.aaz1346

Monaghan MT, Wild R, Elliot M *et al.* Accelerated species inventory on Madagascar using coalescent-based models of species delineation. *Systematic Biology* 2009;**58**:298–311. https://doi.org/10.1093/sysbio/syp027

Myers N, Mittermeier RA, Mittermeier CG *et al.* Biodiversity hotspots for conservation priorities. *Nature* 2000;**403**:853–8. https://doi.org/10.1038/35002501

Oliver LA, Rittmeyer EN, Kraus F *et al.* Phylogeny and phylogeography of *Mantophryne* (Anura: Microhylidae) reveals cryptic diversity in New Guinea. *Molecular Phylogenetics and Evolution* 2013;**67**:600–7. https://doi.org/10.1016/j.ympev.2013.02.023

Oliver PM, Iannella A, Richards SJ *et al.* Mountain colonisation, miniaturisation and ecological evolution in a radiation of direct-developing New Guinea frogs (*Choerophryne*, Microhylidae). *PeerJ* 2017;**23**:e3077.

Oliver PM, Bower DS, McDonald PJ *et al.* Melanesia holds the world's most diverse and intact insular amphibian fauna. *Communications Biology* 2022;**5**:1182. https://doi.org/10.1038/s42003-022-04105-1

Ortiz DA, Hoskin CJ, Werneck FP *et al.* Historical biogeography highlights the role of Miocene landscape changes on the diversification of a clade of Amazonian tree frogs. *Organism Diversity & Evolution* 2023;**23**:395–414.

Padial JM, Miralles A, De La Riva I *et al.* The integrative future of taxonomy. *Frontiers in Zoology* 2010;**7**. https://doi.org/10.1186/1742-9994-7-16

Pons J, Barraclough TG, Gomez-Zurita J *et al.* Sequence-based species delimitation for the DNA taxonomy of undescribed insects. *Systematic Biology* 2006;**55**:595–609. https://doi.org/10.1080/10635150600852011

Portik DM, Streicher JW, Wiens JJ. Frog phylogeny: a time-calibrated, species-level tree based on hundreds of loci and 5,242 species. *Molecular Phylogenetics and Evolution* 2023;**188**:107907. https://doi.org/10.1016/j.ympev.2023.107907

Puillandre N, Lambert A, Brouillet S *et al.* ABGD, Automatic Barcode Gap Discovery for primary species delimitation. *Molecular Ecology* 2012;**21**:1864–77. https://doi.org/10.1111/j.1365-294X.2011.05239.x

Quarles van Ufford A, Cloos M. Cenozoic tectonics of New Guinea. *AAPG Bulletin* 2005;**89**:119–40.

Ree RH, Sanmartín I. Conceptual and statistical problems with the DEC+J model of founder-event speciation and its comparison with DEC via model selection. *Journal of Biogeography* 2018;**45**:741–9. https://doi.org/10.1111/jbi.13173

Ree RH, Smith SA. Maximum likelihood inference of geographic range evolution by dispersal, local extinction, and cladogenesis. *Systematic Biology* 2008;**57**:4–14. https://doi.org/10.1080/10635150701883881

Richards SJ, Oliver PM. A new species of *Hylophorbus* (Anura, Microhylidae) from the Huon Peninsula, Papua New Guinea. *Mitteilungen aus dem Museum für Naturkunde in Berlin – Zoologische Reihe* 2007;**83**:83–9. https://doi.org/10.1002/mmnz.200600030

Rivera JA, Kraus F, Allison A *et al.* Molecular phylogenetics and dating of the problematic New Guinea microhylid frogs (Amphibia: Anura) reveals elevated speciation rates and need for taxonomic reclassification. *Molecular Phylogenetics and Evolution* 2017;**112**:1–11. https://doi.org/10.1016/j.ympev.2017.04.008

Ronquist F. Dispersal–vicariance analysis: a new approach to the quantification of historical biogeography. *Systematic Biology* 1997;**46**:195–203. https://doi.org/10.1093/sysbio/46.1.195

Roycroft E, Fabre PH, MacDonald AJ *et al.* New Guinea uplift opens ecological opportunity across a continent. *Current Biology: CB* 2022;**32**:4215–24.e3. https://doi.org/10.1016/j.cub.2022.08.021

Schenk JJ. Consequences of secondary calibrations on divergence time estimates. *PLoS One* 2016;**11**. https://doi.org/10.1371/journal.pone.0148228

Schneider CA, Rasband WS, Eliceiri KW. NIH Image to ImageJ: 25 years of image analysis. *Nature Methods* 2012;**9**:671–5. https://doi.org/10.1038/nmeth.2089

Shee ZQ, Frodin DG, Cámara-Leret R *et al.* Reconstructing the complex evolutionary history of the Papuasian *Schefflera* radiation through herbariomics. *Frontiers in Plant Science* 2020;**11**:258. https://doi.org/10.3389/fpls.2020.00258

Slavenko A, Tamar K, Tallowin OJS *et al.* Cryptic diversity and non-adaptive radiation of montane New Guinea skinks (*Papuascincus*; Scincidae). *Molecular Phylogenetics and Evolution* 2020;**146**:106749. https://doi.org/10.1016/j.ympev.2020.106749

Smith ML, Noonan BP, Colston TJ. The role of climatic and geological events in generating diversity in Ethiopian grass frogs (genus *Ptychadena*). *Royal Society Open Science* 2017;**4**:170021. https://doi.org/10.1098/rsos.170021

Sueur J, Aubin T, Somonis C. Seewave, a free modular tool for sound analysis and synthesis. *Bioacoustics* 2008;**18**:213–26.

Sukumaran J, Knowles LL. Multispecies coalescent delimits structure, not species. *Proceedings of the National Academy of Sciences of the United States of America* 2017;**114**:1607–12. https://doi.org/10.1073/pnas.1607921114

Tallowin OJS, Tamar K, Meiri S *et al.* Early insularity and subsequent mountain uplift were complementary drivers of diversification in a Melanesian lizard radiation (Gekkonidae: *Cyrtodactylus*). *Molecular Phylogenetics and Evolution* 2018;**125**:29–39. https://doi.org/10.1016/j.ympev.2018.03.020

Tallowin OJS, Meiri S, Donnellan SC *et al.* The other side of the Sahulian coin: biogeography and evolution of Melanesian forest dragons (*Agamidae*). *Biological Journal of the Linnean Society* 2020;**129**:99–113. https://doi.org/10.1093/biolinnean/blz125

Toussaint EFA, Hall R, Monaghan MT *et al.* The towering orogeny of New Guinea as a trigger for arthropod megadiversity. *Nature Communications* 2014;**5**:4001. https://doi.org/10.1038/ncomms5001

Toussaint EFA, White LT, Shaverdo H *et al.* New Guinean orogenic dynamics and biota evolution revealed using a custom geospatial analysis pipeline. *BMC Ecology and Evolution* 2021;**21**:51. https://doi.org/10.1186/s12862-021-01764-2

Tu N, Yang M, Liang D *et al.* A large-scale phylogeny of Microhylidae inferred from a combined dataset of 121 genes and 427 taxa. *Molecular Phylogenetics and Evolution* 2018;**126**:85–91. https://doi.org/10.1016/j.ympev.2018.03.036

Unmack PJ, Allen GR, Johnson JB. Phylogeny and biogeography of rainbowfishes (Melanotaeniidae) from Australia and New Guinea. *Molecular Phylogenetics and Evolution* 2013;**67**:15–27. https://doi.org/10.1016/j.ympev.2012.12.019

Utami CY, Sholihah A, Condamine FL *et al.* Cryptic diversity impacts model selection and macroevolutionary inferences in diversification analyses. *Proceedings Biological Sciences* 2022;**289**:20221335. https://doi.org/10.1098/rspb.2022.1335

Vacher J, Chave J, Ficetola FG *et al.* Large-scale DNA-based survey of frogs in Amazonia suggests a vast underestimation of species richness and endemism. *Journal of Biogeography* 2020;**47**:1781–91. https://doi.org/10.1111/jbi.13847

van Ginneken M, Decru E, Verheyen E *et al.* Morphometry and DNA barcoding reveal cryptic diversity in the genus *Enteromius* (Cypriniformes: Cyprinidae) from the Congo basin, Africa. *European Journal of Taxonomy* 2017;**310**:1–32. https://doi.org/10.5852/ejt.2017.310

Vences M, Vieites DR, Glaw F *et al.* Multiple overseas dispersal in amphibians. *Proceedings of the Royal Society B: Biological Sciences* 2003;**270**:2435–42. https://doi.org/10.1098/rspb.2003.2516

Vences M, Thomas M, van der Meijden A *et al.* Comparative performance of the 16S rRNA gene in DNA barcoding of amphibians. *Frontiers in Zoology* 2005;**2**:5. https://doi.org/10.1186/1742-9994-2-5

Vieites DR, Wollenberg KC, Andreone F *et al.* Vast underestimation of Madagascar's biodiversity evidenced by an integrative amphibian inventory. *PNAS* 2009; **106**: 8267–8272. https://doi.org/10.1073/pnas.0810821106

Watters JL, Cummings ST, Flanagan RL *et al*. Review of morphometric measurements used in anuran species descriptions and recommendations for a standardized approach. *Zootaxa* 2016;**4072**:477–95.

Webb M, White LT, Jost BM *et al*. The Tamrau Block of NW New Guinea records late Miocene–Pliocene collision at the northern tip of the Australian Plate. *Journal of Asian Earth Sciences* 2019;**179**:238–60. https://doi.org/10.1016/j.jseaes.2019.04.020

Zeisset I, Beebee TJC. Amphibian phylogeography: a model for understanding historical aspects of species distributions. *Heredity* 2008;**101**:109–19. https://doi.org/10.1038/hdy.2008.30

Zhang J, Kapli P, Pavlidis P *et al*. A general species delimitation method with applications to phylogenetic placements. *Bioinformatics* 2013;**29**:2869–76. https://doi.org/10.1093/bioinformatics/btt499

Zweifel RG. A revision of the frogs of the subfamily Asterophryinae family Microhylidae. *Bulletin of the American Museum of Natural History* 1972;**148**:411–546.